Immune profiling of peripheral blood NKG2D+ cytotoxic lymphoid cells reveals systemic immune shifts in active alopecia areata

Chung, Kyung Bae

Department of Medicine

Graduate School

Yonsei University

Immune profiling of peripheral blood NKG2D+ cytotoxic lymphoid cells reveals systemic immune shifts in active alopecia areata

Advisor Kim, Do-Young

A Dissertation Submitted

to the Department of Medicine

and the Committee on Graduate School

of Yonsei University in Partial Fulfillment of the

Requirements for the Degree of

Doctor of Philosophy in Medical Science

Chung, Kyung Bae

June 2025

Immune profiling of peripheral blood NKG2D+ cytotoxic lymphoid cells reveals systemic immune shifts in active alopecia areata

This Certifies that the Dissertation of Chung, Kyung Bae is Approved

Committee Chair	**Kim, Tae-Gyun**
Committee Member	**Kim, Do-Young**
Committee Member	**Hong, Seunghee**
Committee Member	**Shin, Ha Young**
Committee Member	**Cho, Hyunsoo**

Department of Medicine
Graduate School
Yonsei University
June 2025

ACKNOWLEDGEMENTS

I would like to thank all the people who have helped and inspired me during my doctoral study.

First and foremost, I offer my sincere gratitude to my supervisor, Professor Do-Young Kim, whose patience and warm consideration have inspired me throughout my doctoral dissertation. His expertise and dedication have been invaluable to this study. More than just a teacher, he has been a mentor in both my academic and personal growth.

I also extend my appreciation to Professor Tae-Gyun Kim, Professor Ha Young Shin, Professor Hyunsoo Cho, and Professor Seunghee Hong who gave me experienced advice and support.

My sincere thanks go to Ms. Ji Hye Hwang and Ms. Eun Hye Kim for their tremendous help during extensive experiments. I am also grateful to my colleague, Hee Ung Park, for his support and collaboration throughout many aspects of my research.

Finally, my deepest gratitude goes to my family. This dissertation has been possible due to my family's love, endurance and unwavering support. I would like to thank my wife, Wonju, and my beloved child, Hyunmin, for bringing joy to my life and helping me stay courageous in the face of challenges. Also, I would like to thank my mom and dad for their endless support, giving me confidence and encouragement. I would also like to thank my parents-in-law for their substantial assistance and support.

TABLE OF CONTENTS

LIST OF FIGURES

LIST OF TABLES

ABSTRACT

Immune profiling of peripheral blood NKG2D+ cytotoxic lymphoid cells reveals systemic immune shifts in active alopecia areata

Alopecia areata (AA) is a chronic autoimmune disease characterized by recurrent hair loss due to the breakdown of immune privilege in hair follicles. This breakdown leads to the expression of Natural Killer Group 2 member D (NKG2D) ligands (e.g.ULBP3), which cause immune-mediated follicular attack. Among immune cells, NKG2D+ CD8+ T cells play a key pathogenic role in AA, as demonstrated in mouse models. While these cells are also implicated in human AA, differences in NKG2D expression make the role of these cells remain elusive.

Recent studies suggest that AA involves systemic immune dysregulation beyond skin, with inflammatory signals in affected skin correlating with those in blood. Some studies have reported increased expression of NKG2D in lymphoid cell subsets, including CD4+ and CD8+ T cells as well as CD56+ NK cells, in the blood of AA patients compared to healthy controls. Environmental triggers such as vaccinations, viral infections, and allergies have been associated with disease aggravation, suggesting a shift in systemic immune alteration rather than direct effect on skin.

From this background, it was hypothesized that NKG2D+ cells in human blood would show immune shifts between different AA disease states, requiring a high-resolution evaluation of these cells. Also, since NKG2D has different features in human compared to animals, evaluation on NKG2D+ cells was required.

To investigate changes in NKG2D+ cells and their correlation with disease severity and activity in AA, peripheral blood mononuclear cells (PBMCs) were collected from patients and analyzed for NKG2D+ lymphoid subsets, including CD4, CD8, NK (CD3−, CD56+), and CD3+CD56+ cells. The proportions of each subset, as well as NKG2D+ cells, showed no significant differences between AA patients and healthy controls, and no correlation with disease severity or activity was observed.

Given the interpersonal variation in immune cell composition, a paired analysis was conducted using samples from individual patients in active and stable disease states. NKG2D+ cells were sorted and analyzed using single-cell RNA sequencing (scRNA-seq) to enable a higher-resolution characterization of immune changes. Among the four major lymphoid subsets (CD8+ T cells, NK cells, mucosal-associated invariant T (MAIT) cells, and γδ T cells), an increased proportion of NKG2D+ NK cells and a decreased proportion of NKG2D+ CD8+ T cells were identified in the active disease state. Notably, cytotoxic CD8+ T cell subsets (GZMK+ and GZMB+) were enriched during active disease. Unsupervised differential abundance analysis using MILO further confirmed the increase of GZMK+ T cells. These changes were validated by flow cytometry, which revealed a specific increase in GZMK+ Temra cells.

Transcriptomic analysis indicated enhanced activation and cytotoxicity of T cells in the active phase. Upstream regulator analysis using Ingenuity Pathway Analysis (IPA) identified cytokines as potential drivers of these changes. However, subsequent evaluation of cytokine levels by ELISA and bulk RNA sequencing of blood monocytes did not reveal significant differences between disease states.

In conclusion, while the overall proportions of NKG2D+ lymphoid cells did not differ significantly between AA patients and healthy controls, a more detailed analysis revealed shifts toward cytotoxic T cell and NK cell expansion in active AA. Although cytokines were identified as potential upstream drivers of the immune shift, no significant differences were observed in serum cytokine levels or in the activity of cytokine-producing innate immune cells. These findings suggest the possibility of a tissue-originated signal; however, further investigation is required to elucidate the underlying source of immune modulation.

Keywords : Alopecia areata, NKG2D, Cytotoxic T cells

Immune profiling of peripheral blood NKG2D+ cytotoxic lymphoid cells reveals systemic immune shifts in active alopecia areata

1. INTRODUCTION

Alopecia areata(AA) is an autoimmune disorder, leading to hair loss with collapse of immune privilege of hair follicles and autoimmune attack.[1] Due to the chronic immunologic process of disease, immunomodulating features using corticosteroids or immunosuppressants have been used as traditional treatment methodologies. New therapeutic strategies, such as JAK inhibitors, have overcome therapeutic challenges in a considerable portion of patients with alopecia areata, but there remain patients who do not respond to these novel therapeutics and inflammatory process driving alopecia areata remains unclear.[2, 3] From past experiments, hair follicles were identified as immune-privileged organs.[4, 5] Restricted immune cell recruitment/trafficking, reduced antigen presentation and active immunosuppression with immune modulatory signals are known as the principal immune privilege mechanisms.[6] However, AA involves the breakdown of immune-privilege, leading to inflammation around hair follicles leading to hair loss.[6] Two core theories explain the onset of breakdown in immune privilege; (1) Local disturbance in hair follicles as initiators of immune privilege collapse and (2) The hair follicle as an innocent bystander in a dysregulated immune system. CD8 T cells which lead to the collapse in immune privilege are regarded as the pathogenic cells in AA.[7]

The pathogenic CD8 T cells express NKG2D receptors, which are activating receptors that belong to the NKG2 family. The role of NKG2D in AA was first identified in a previous genome wide association(GWAS) study, which established the genetic basis of AA in 2010.[8] This study revealed regions associated to AA, which were genes related to antigen presentation, function of regulatory T cells, chemokine and chemokine receptors, oxidative stress and NKG2D activating ligands.[8-10] Moreover, within the study, AA hair follicles, in contrast to normal hair follicles, expressed higher level of NKG2D ligands (ULBP3) leading to infiltration of NKG2D+CD8 T cells.[8] Later, in an animal study, NKG2D+ cytotoxic T cells was identified as the main contributors of disease. Infiltration of NKG2D+ CD8 T cells were found to be indispensable and sufficient for the induction of disease in spontaneously disease developing C3H/HeJ mouse models.[1, 11] When NKG2D was depleted, induction of AA was unattainable. Tissue infiltrated CD8+NKG2D+ T cells express genes related to an inflammatory cascade, causing increase of interferon (IFN) response genes, cytotoxic T cell (CTL)-specific transcripts and transcripts for IL-12 and IL-15 in the skin of AA.[12]

NKG2D, encoded by *KLRK1*, is an activating cell surface receptor that is usually expressed on immune cells with cytotoxicity. [13] NKG2D is expressed on NK cells, NKT cells, γδ T cells, CD8 T cells and a subset of CD4 T cells. The NKG2D is documented as a co-stimulatory molecule for T cells, and upon engagement of NKG2D ligands(NKG2DL), stimulated human CTL cells produce cytokines such as IFN-γ, TNF and IL-2 in response to TCR stimulation and show increased cytolytic response. [13, 14] Unlike restricted expression of NKG2D on 'activation of CD8 T cells' in mouse, human CTLs broadly express NKG2D, even in a naïve status. [15] Therefore, despite NKG2D+ cytotoxic T cells infiltrate around hair follicles of AA patients, the fact that NKG2D is expressed on most CTLs raises the question of whether NKG2D is a bystander receptor or the morbific receptor. [16, 17] So far, evidences supporting direct pathogenic role of NKG2D-expressing cells in human alopecia areata is relatively insufficient compared with CH3/HEJ mouse models. [18]

Recent studies on the epidemiologic characteristics have found that alopecia areata is a systemic disorder with diverse comorbidities. [19, 20] Many studies identified systemic inflammation with increased inflammatory blood parameters and proteins related to the pathogenic cascade. [21-24] Moreover, studies have shown that the inflammatory status of the scalp and the blood correlates, suggesting that markers from the serum can reflect the inflammatory condition of hair follicles. [22]

Also, studies have shown that AA can be aggravated with change in systemic conditions including viral infection, vaccination and allergic influence; especially during the COVID-19 era. [20, 25-27] Although the systemic inflammatory characteristic of disease is recently emphasized, blood studies for specific immune cells is less established. Earlier studies on the blood immune cells have focused on NKG2D+ cells and shown increases in NKG2D+ CD4+ cells, CD8+ cells and NK cells in alopecia areata patients compared to healthy control. [28] In addition, NKG2D was significantly upregulated on blood CD56+NK cells and CD8+ T cells in AA. [17] However, these results were not evaluated with the correlation of clinical parameters of AA patients.

From this background, I hypothesized that NKG2D+ cells in blood of AA would change between the clinical status of AA. This study aims to observe the phenotypes of NKG2D+ cells in AA and to elucidate the change in NKG2D+ cells within the changing status of AA.

2. MATERIALS AND METHODS

2.1. Study subjects

2.1.1. Clinical information

Clinical information from patients who have donated blood were achieved including sex, age, onset age of AA, severity of alopecia score (SALT) score, activity of disease and history of disease was gathered in the study.

2.1.2. Disease activity of alopecia areata

The disease activity of alopecia areata was evaluated through patient history, medication response, hair pull test and dermoscopic evaluation. Patients exhibiting clinical markers of disease progression (dermoscopic signs of broken hair, black dots, exclamation hair) and positive hair pull test were classified as ‘highly active’. Those with an active status with mixed regrowing pattern as ‘borderline activity’ and no signs of clinical activity with regrowing hair status as having ‘stable disease’.

2.2. Peripheral blood samples

2.2.1. Sample collection

Blood samples were collected from patients diagnosed with chronic alopecia areata, characterized by consistent relapse. Healthy control patients donated blood with arbitrary consent. Patient’s blood was not collected if the patient had symptoms of viral infection, history of cancer or other autoimmune disorders. The samples were obtained after receiving informed consent from all participants, in accordance with a protocol approved by the Yonsei University College of Medicine Institutional Review Board (IRB No. 4-2020-1372). All procedures involving human subjects were conducted in adherence to the ethical principles outlined in the Declaration of Helsinki.

2.2.2. Collection timepoints

Blood samples were primarily collected when patients were in the ‘active status’ of alopecia areata, defined by the presence of ongoing hair loss. If the patient responded successfully to treatment and transitioned to a ‘stable status,’ defined by the cessation of new hair loss and signs of hair regrowth, an additional blood sample was retrieved for comparative analysis. Patients who were at the ‘stable status’ at the primary collection and aggravated within a timepoint were also included in the study.

2.2.3. Sample Processing

Upon collection, blood samples were processed immediately to ensure cell viability and minimize degradation. Peripheral blood mononuclear cells (PBMCs) and plasma were separated using density gradient centrifugation with Ficoll-Paque PLUS (Cytiva, #17144002, Piscataway, NJ, USA) from heparinized peripheral blood. The samples were centrifuged at 400 × g for 30 minutes at room temperature without braking to separate the PBMC layer. The mononuclear cells were then carefully aspirated, washed twice in phosphate-buffered saline (PBS), and resuspended in a freezing medium consisting of 90% fetal bovine serum (FBS) and 10% dimethyl sulfoxide (DMSO) before being stored in liquid nitrogen or – 70℃ deep freezer for future analysis. Blood plasma was obtained and stocked separately from PBMCs.

2.3. Flow cytometry analysis of PBMCs.

2.3.1. Panel design

A flow cytometry panel was designed to evaluate NKG2D expression and immune cell phenotypes, and cytotoxicity of cells. The panel included the following antibodies and fluorochromes.

Panel for NKG2D expressing lymphoid cells, comparison with healthy control samples					
	Fluorescence	Antibody	Manufacturer	Catalog #	Clone #
1	FITC	CFSE	Invitrogen		
2	BV510	Zombie Aqua	Biolegend	423102	
3	BV650	CD3	Biolegend	317324	OKT3
4	BV785	CD4	Biolegend	300554	RPA-T4
5	BV421	CD8a	Biolegend	301036	RPA-T8
6	APC	CD14	Biolegend	301808	M5E2
7	BV605	CD16	Biolegend	302040	3G8
8	Alexa Fluor 700	CD56	BD Pharmingen	557919	B159
9	PE	CD314(NKG2D)	Biolegend	320806	1D11
10	Alexa Fluor 647	CLA	Biolegend	321309	HECA-452

Panel for Paired samples					
	Fluorescence	Antibody	Manufacturer	Catalog #	Clone #
1	APC-Cy7	Zombie NIR	Biolegend	423106	
2	BUV395	CD45	BD Horizon™	563792	H130
3	BV650	CD3	Biolegend	317324	OKT3
4	BV786	CD4	Biolegend	300554	RPA-T4
5	BB700	CD8	BD Horizon™	566452	PRA-T8
6	RB780	CD56	BD Horizon™	568763	B159
7	FITC	TCR gd	BD Pharmingen™	559878	B1
8	APC	TCR Va7.2	Biolegend	351708	3C10
9	PE	NKG2D	Biolegend	320806	1D11

Panel for Cytotoxicity(ICS)					
	Fluorescence	Antibody	Manufacturer	Catalog #	Clone #
1	APC-Cy7	Zombie NIR	Biolegend	423106	
2	BV605	CD45RO	BD Horizon™	562791	UCHL1
3	BV650	CD3	Biolegend	317324	OKT3
4	BB700	CD8	BD Horizon™	566452	PRA-T8
5	RB780	CD56	BD Horizon™	568763	B159
6	BUV395	CCR7	BD Horizon™	568681	3D12
7	PE	NKG2D	Biolegend	320806	1D11
8	BV711	HLA-DR	Biolegend	307644	L243
9	AF647	Granzyme K	BD Pharmingen™	566655	G3H69
10	AF488	Granzyme B	Invitrogen	MA5-23639	351927

2.3.2. Staining protocol

2.3.2.1. Sample preparation

Cryopreserved PBMCs were thawed in 37℃ water bath. A total of 1 ml pre-warmed RPMI containing 10% FBS and 1% Antibiotic-Antimycotic was added. The PBMCs were then transferred to a 15 ml conical tube. Cells were centrifuged at 350 g for 5 min at 4 ℃.

2.3.2.2 Surface marker staining

The thawed PBMCs were resuspended and adjusted to a concentration of 1–2 × 10^6 cells/200 µl in cold PBS with 1% FBS, then transferred to a V-bottom 96-well plate. To distinguish live and dead cells, the cells were stained with Zombie NIR (Biolegend, San Diego, CA, USA, #423106) for 15 min at room temperature, protected from light. An antibody cocktail was prepared in cold PBS with 1% FBS and Brilliant Stain Buffer Plus (BD Biosciences, San Jose, CA, USA, #566385). The PBMCs were incubated with the antibody cocktail on ice for 25 min, protected from light. After incubation, PBMCs were washed twice with cold PBS containing 1% FBS.

2.3.2.3 Intracellular staining

To detect intracellular cytokines, thawed PBMCs were stimulated with 50 ng/mL Phorbol 12-myristate 13-acetate (PMA) and 1 µg/mL Ionomycin, followed by treatment with GolgiPlug (BD Biosciences, San Jose, CA, USA, #555029) and GolgiStop (BD Biosciences, San Jose, CA, USA, #554724) in RPMI containing 10% FBS and 1% AA. The PBMCs were then seeded into a 24-well non-treated plate and incubated for 5 hours at 37°C in a CO_2 incubator. After surface staining, the PBMCs were fixed and permeabilized using Fixation and Permeabilization Solution (BD Biosciences, San Jose, CA, USA, #554722) and washed with 1X Perm/Wash Buffer (BD Biosciences, San Jose, CA, USA, #554723) diluted in distilled water. The permeabilized PBMCs were then stained for intracellular stains on ice for 25 min, protected from light. After incubation, PBMCs were washed twice with 1X Perm/Wash Buffer.

2.3.3. Acquisition of Stained Cells and Analysis

Stained cells were acquired using an LSR II (BD Biosciences, San Jose, CA, USA), Symphony A5(BD Biosciences, San Jose, CA, USA) and Symphony A5 SE (BD Biosciences, San Jose, CA, USA) flow cytometer. Data acquisition was performed using BD FACSDiva software, ensuring proper instrument calibration and compensation settings. All flow cytometry data were analyzed using FlowJo software (Treestar, Ashland, OR, USA). Doublet discrimination, viability gating, and sequential gating strategies were applied to identify immune cell populations and assess NKG2D expression patterns.

2.3.4. Statistical Analysis

Statistical comparisons of cell proportions between different disease activity states were performed using paired t-tests or Wilcoxon signed-rank tests, depending on data normality. A p-value of <0.05 was considered statistically significant. Data visualization was conducted using GraphPad Prism 10 or R software.

2.4. scRNA sequencing, Multiplex scRNA sequencing.

2.4.1. Composition of scRNA-seq and Multiplex scRNA-seq data

A total of 10 samples, consisting of five patient pairs classified as 'active' and 'stable' (N=5), were included in the scRNA sequencing analysis. Single-cell suspension was prepared by thawing frozen PBMCs. Among total of 10 paired samples, 6 underwent standard scRNA-seq, while 4 were processed using multiplexed scRNA-seq. Each single cell suspension was stained with NKG2D and DAPI.

2.4.2. Standard scRNA-seq

A total of six patient samples underwent standard scRNA-seq in two different batches. Each single-cell suspension was thawed and stained with NKG2D and DAPI, and live NKG2D+ cells were sorted using a sorter (BD FACS Aria III (BD Biosciences, San Jose, CA, USA)). Sorted live cells were processed using the 10x Genomics Chromium system, and cDNA libraries were generated with the Chromium Next GEM Single Cell 5p RNA library v1.1 (10x Genomics, Pleasanton, CA) according to the manufacturer's protocol. Barcoded libraries were sequenced with the Hi-Seq X Ten platform (Illumina), and raw data were processed using the standard Cell Ranger pipeline v6.1.2 (10x Genomics). Analysis of raw gene expression matrices was performed by Seurat software v4.1.0 following a standard workflow. [29]

2.4.3. Multiplex hashtag oligo scRNA-seq

Among total of 10 paired samples, four of them were processed using multiplexed scRNA-seq. Each single cell suspension was thawed and primarily stained with hashtag oligo (HTOs) for each sample. Then each sample was stained with NKG2D (Biolegend, San Diego, CA, USA #320806) and Live/Dead (FVS700 (BD Biosciences, San Jose, CA, USA, #564997)). After staining, the samples were pooled with the same same number of cells for each sample (10 $x10^5$ cells). After pooling, live, NKG2D+ cells were sorted using a cell sorter (BD Symphony S6). Sorted live cells were processed using the 10x Genomics Chromium system, and cDNA libraries were generated with the Chromium Next GEM Single Cell 5' Reagent Kits v2 (Dual Index) (10x Genomics, Pleasanton, CA) according to the manufacturer's protocol. Barcoded libraries were sequenced with the Novaseq 6000 platform, and raw data were processed using the standard Cell Ranger pipeline v7.1.0 (10x Genomics). Analysis of raw gene expression matrices was performed by Seurat software v4.1.0 following a standard workflow. [29]

2.4.4. TCR V(D)J sequencing and analysis

Full-length TCR V(D)J segments were achieved from cDNA using a Chromium Single-Cell V(D)J Enrichment kit according to the manufacturer's protocol (10x Genomics). Sequencing libraries were prepared in a 3-nM concentration and then sequenced on a Hi-Seq X Ten (lllumina) or Novaseq 6000 platform with 150-bp paired-end reads. Demultiplexing, gene quantification and TCR clonotype assignment were performed using CellRanger v.2.1.1 (10x Genomics). Analysis was performed using scRepertoire package v.1.12.0. [30]

2.4.5. Packages and software

In the analysis, I included cells, which met filtration criteria, (1) the number of genes higher than > 250, (2) UMI counts >=500, (3) <10% of mitochondrial gene expression, and performed normalization, integration, and scaling using Seurat package v4.1.0. [29] Using Doubletfinder, I have removed suggestive doublet cells. [30] Cells were clustered by principal component analysis(PCA) followed by Seurat FindCluster function with resolution of 1.0. [29] Cellular annotation was performed by unbiased approaches based on the profiling of differentially expressed genes (DEGs) for each cluster using Seurat FindMarkers function, which presented several cell type-specific genes to define cell identity. Subset analysis for the CD8 T cell cluster was performed according to the standard pipeline applied to the whole cells.

2.5. Evaluation of cell proportion in scRNA-seq data

Cell proportion analysis was performed to assess differences in cellular composition between the 'active' and 'stable' groups in the scRNA-seq dataset. The analysis was conducted for two datasets; (1) Total dataset including all NKG2D+ cells (2) Subset analysis of NKG2D+ CD8 T cells, which are known as main pathogenic cells. Cell population was calculated as percentage of cells within the total number of captured cells. Proportional plot was drawn based on the cell proportion of all samples. For statistical analysis, considering the paired samples from the same individual, a paired t-test was used to assess whether differences in cell proportions between the 'active' and 'stable' states were statistically significant. This approach ensured that inter-individual variability was controlled, allowing for a more accurate evaluation of differential cell representation across conditions.

2.6. Differential abundance analysis

Unsupervised differential abundance analysis was done using MILO v1.10.0, which is a method that enables the detection of differentially abundant cell populations while accounting for the complex structure of single-cell data. [31] MILO object was constructed based on PCA. Neighborhood graphs were constructed from the integrated dataset, and neighborhoods were assigned weights based on their local cell densities (prop = 0.2). A generalized linear model was applied to test for

differential abundance between the 'active' and 'stable' groups. neighborhoods displaying significant differential abundance are colored by their log-Fold Change. This approach allowed for a robust identification of shifts in cell population, minimizing biases associated with predefined cluster annotations.

2.7. Pathway analysis with Metascape functional tool

Pathway enrichment analysis was performed to identify biological processes and signaling pathways associated with differentially expressed genes (DEGs) in T cells. The analysis was conducted using the web-based Metascape functional annotation tool, which integrates multiple pathway databases, including KEGG, GO Biological Processes, Reactome, and others, to provide comprehensive functional insights.[32] DEGs were defined by using FindMarkers function comparing T cells' 'active' and 'stable' status with criteria using log2 fold-change (Log2FC)≥ 0.5 and an adjusted p-value < 0.05.

2.8. Ingenuity pathway analysis (IPA)

Ingenuity pathway analysis (IPA) was used to identify upstream regulators and signaling pathways responsible for the observed changes in T cells. This analysis aimed to predict the key molecular drivers influencing differential gene expression between the 'active' and 'stable' states of CD8 T cells. Obtained differentially expressed genes (DEGs) by comparing 'active' and 'stable' status of CD8 T cells (adjusted p-value < 0.05, Log2FC > 0.5) were used for input data for IPA. I analyzed the 'upstream regulators' contributing to the observed gene expression patterns. Categories with a Z-score > 2.0, indicating significant pathway activation, were included in the result.[33]

2.9. Enzyme-Linked Immunosorbent Assay

Blood plasma samples were used to quantify Interleukin-15 (IL-15) levels and assess differences between the 'active' and 'stable' states. IL-15 concentrations were measured using the Human IL-15 ELISA Kit (Invitrogen, Carlsbad, CA, USA) following the manufacturer's protocol. The assay was performed by adding plasma samples to ELISA plates pre-coated with IL-15 capture antibodies, followed by incubation with detection reagents. Absorbance was measured at 450 nm VersaMAX microplate reader (Molecular Devices). The concentration of IL-15 in each sample was determined by interpolating absorbance values against a standard curve generated from known IL-15 concentrations.

2.10. Bulk RNA sequencing on monocytes

To evaluate the transcriptomic changes in monocytes, HLA-DR+, CD14+ cells were sorted from PBMC. Blood was thawed and incubated at room temperature overnight. When incubated, HLA-DR (PerCP-Cyanin5.5, Invitrogen, # 45-9956-42), CD14 (APC, Biolegend, #301808) was used to stain monocytes. These cells were sorted using a FACS Aria III sorter (BD Biosciences, San Jose, CA, USA). RNA was extracted according to manufacturer instructions. A total of 6 samples (3 paired) passed the quality control and analyzed. DESeq2 was used for analysis. I filtered out low counts of genes below 100 and sum value below 500. A total for 8,598 genes were used for further analysis.

2.11. Statistical analysis

Data were analyzed with Student's t-tests, unless otherwise stated, using Prism 10 software (GraphPad Software Inc., San Diego, CA, USA). Analysis of variance (ANOVA) with Bonferroni correction was used for multiple comparisons. All *P*-values < 0.05 were considered statistically significant.

3. RESULTS

3.1. NKG2D+ cell percentage between AA patients and healthy control

To evaluate the baseline level of NKG2D+ cells and compare with healthy controls, I analyzed the proportions of lymphoid subtypes, the overall percentage of NKG2D+ expression, and the proportion of NKG2D-expressing subsets among total lymphoid cells in fourty-seven AA patients. No differences were identified in percentage of CD4, CD8, NK (CD3-, CD56+), CD3+CD56 + cells among total lymphoid cells (Figure 1A). The proportion of NKG2D expressing cells were assessed, revealing a higher percentage in NK (CD3-, CD56+) cells and a lower percentage in CD3+CD56+ cells in AA (Figure 1B). The expression was not different in CD8 T cells nor CD4 T cells. Also, the overall proportion of NKG2D+ cells among total lymphoid cells did not reveal any differences (Figure 1C).

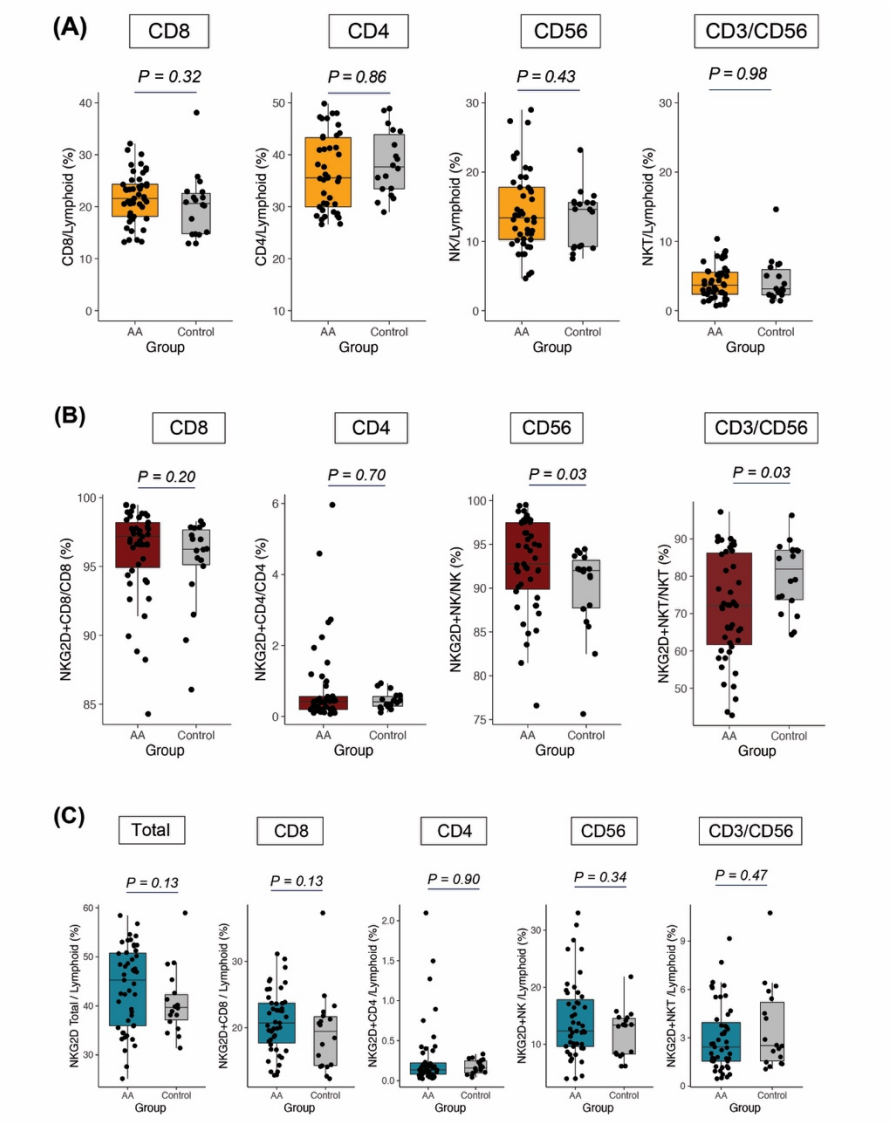

Figure 1. Analysis of NKG2D+ cells among lymphoid cells in human PBMCs.
Proportions of lymphoid subtypes, the overall percentage of NKG2D+ expression, and the proportion of NKG2D-expressing subsets among total lymphoid cells were analyzed. (n=47 AA patients, n=18 healthy control) (A) Lymphoid cell type percentage among total lymphoid cells do not show differences between AA and healthy control. (B) NKG2D expression percentage is increased in AA NK cells and decreased in CD3+CD56+ cells. (C) NKG2D+ lymphoid cell subtypes among total lymphoid cells do not show statistical significance.

Table 1. Clinical and demographic information of alopecia areata patients included in the flow cytometry analysis with comparisons to healthy controls.

Status	Age	Sex	Activity	SALT score	Type of AA
Active	27	M	Mild	30	Patchy AA
Active	28	M	Mild	20	Patchy AA
Active	18	M	Mild	10	Patchy AA
Active	25	M	Mild	20	Patchy AA
Active	25	M	Mild	40	Patchy AA
Active	23	M	Mild	80	Alopecia Totalis
Active	23	F	Mild	75	Alopecia Totalis
Active	58	F	Mild	25	Patchy AA
Active	62	M	Mild	100	Alopecia Universalis
Active	53	F	Severe	87.5	Alopecia Totalis
Active	44	F	Mild	100	Alopecia Universalis
Active	30	F	Severe	30	Patchy AA
Stable	52	F	Stable	3	Patchy AA
Active	45	F	Mild	3	Ophiasis
Active	30	F	Severe	100	Acute Diffuse Total alopecia
Stable	47	M	Stable	25	Patchy AA
Active	43	M	Severe	80	Patchy AA
Active	47	M	Mild	25	Patchy AA
Active	44	F	Severe	100	Alopecia Universalis
Active	44	F	Severe	90	Alopecia Universalis
Active	42	M	Mild	6	Patchy AA
Stable	28	F	Stable	4	Patchy AA
Active	44	F	Mild	8	Patchy AA
Active	29	M	Mild	97.5	Alopecia Universalis
Active	43	M	Severe	6	Patchy AA

Active	25	F	Severe	100	Alopecia Universalis
Active	29	F	Severe	98	Acute Diffuse Total alopecia
Active	24	M	Severe	8	Patchy AA
Active	44	F	Mild	15	Patchy AA
Active	47	F	Mild	30	Patchy AA
Active	47	M	Mild	10	Patchy AA
Active	19	M	Mild	100	Alopecia Universalis
Active	22	F	Mild	25	Patchy AA
Active	45	F	Severe	19	Patchy AA
Active	29	F	Severe	30	Patchy AA
Stable	50	F	Stable	3	Patchy AA
Active	46	F	Mild	10	Patchy AA
Active	38	F	Severe	75	Patchy AA
Active	36	M	Severe	90	Alopecia Totalis
Active	22	F	Mild	25	Patchy AA
Active	43	M	Severe	90	Alopecia Totalis
Active	39	M	Mild	90	Alopecia Universalis
Active	25	M	Mild	100	Alopecia Universalis
Active	45	F	Severe	50	Patchy AA
Active	61	F	Mild	15	Patchy AA
Active	39	F	Mild	30	Ophiasis
Active	39	F	Mild	30	Patchy AA

AA, alopecia areata; SALT, severity of alopecia tool

3.2. Correlation between NKG2D+ cells and clinical characteristics of alopecia areata

To identify the relationship of NKG2D+ cells within alopecia areata patients, I have evaluated the severity and activity of alopecia areata in patients and compared it with the NKG2D+ cell percentage among lymphoid cells. Since NKG2D+ CD8 T cells are suggested to be pathogenic and NKG2D expression is increased in NK cells, evaluation focused on the change within CD8 T cells and NK cells. The percentage of NKG2D+ CD8 T cells (p = 0.82, R = -0.033) nor NKG2D+ NK cells (p = 0.86, R = -0.026) correlated with SALT score (Figure 2A). Additional assessment of activity and the cell proportion showed a mild increase in NKG2D+ NK cells with a slight decrease in NKG2D+ CD8 T cells at a high activity status, however, did not show statistical meaningful changes (Figure 2B). This may have been due to individual immunologic characteristics.

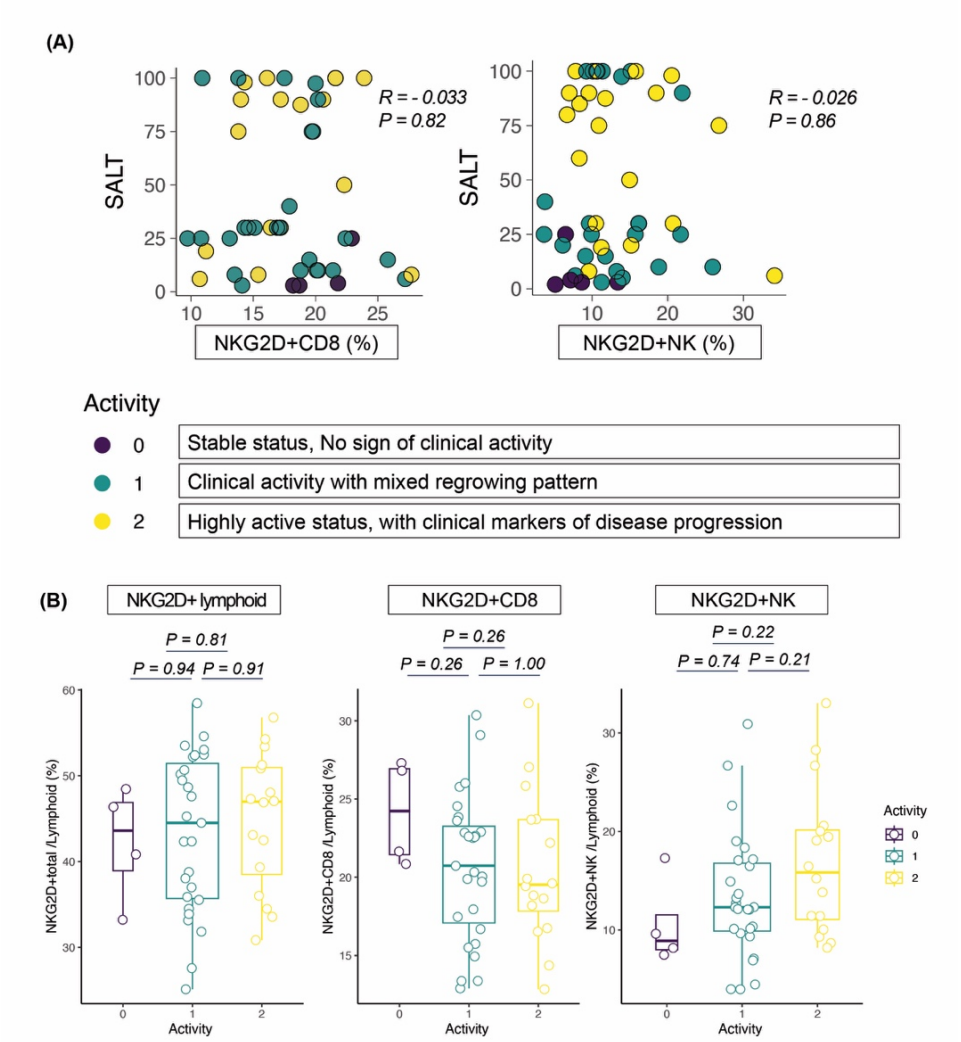

Figure 2. Correlation of NKG2D+ lymphoid cell proportion with severity and activity of alopecia areata. (A) Evaluation of severity of alopecia areata using SALT score and correlation with NKG2D+ CD8, NK cells. No statistical correlation was identified between severity of AA and NKG2D+ lymphoid cell proportion. (B) Activity of disease assessment and correlation with percentage of NKG2D+ CD8, NK cells. No statistical difference was identified between activity of AA and NKG2D+ lymphoid cell proportion.

3.3. Overall composition change of NKG2D+ cells in scRNA-seq data set

Since NKG2D+ lymphoid cells do not show difference between AA patients and healthy control, and does not correlate with severity nor activity, I have tried to evaluate the NKG2D+ cells at a higher resolution in blood. To explore NKG2D+ cells in a deeper scope of view, I isolated NKG2D-positive cells and performed scRNA-seq analysis on the sorted population. Since there is an inherent variability in immune cell composition across individuals, I focused on a paired samples from each patient, comparing their active and stable disease states. Only patients with a SALT score above 50 during the active phase were included, and blood was re-collected during the stable phase, at least one month after discontinuing all medications. The study included 5 patients, with 10 paired samples (active and stable). In the active status, patients showed an average SALT score of 70 (standard deviation (SD):14.1) in the active status. In the stable status, all patients had been in a resolution status with minimal, regrowing alopecic lesions. (Table 2).

Within the scRNA-seq data set, a total of 77,942 cells were included (Figure 3A). A UMAP plot identified four major NKG2D+ cell subsets including T cells, NK cells, γδTcells and Mucosal-associated invariant (MAIT) cells (Figure 3B, C). Cells sorted using the NKG2D antibody exhibited high gene-level expression of *KLRK1* (NKG2D) (Figure 3D). Among these sorted cells, *KLRK1*-expressing cells accounted for 72.2% of T cells, 80.7% of NK cells, 51.9% of MAIT cells, and 75.1% of γδ T cells, suggesting mild discrepancy between protein expression and transcriptomic levels (Figure 3E).

In the comparison between active and stable status of each sample, T cell proportion showed a statistically significant decrease in the active state ($p = 0.014$), with 50.3% (SD: 8.8%) in the active status compared to 59.6% (SD: 9.9%) in the stable status (Figure 3F, G, H) among sorted NKG2D+ cells. Conversely, NK cells were significantly increased in the active state ($p = 0.021$), with 35.1% (SD 14.9) in the active state versus 26.6% (SD: 12.5) in the stable state. MAIT cells and γδT cells did not show statistical difference.

Table 2. Clinical information and activity status of patient samples included in the scRNA-seq analysis

Patient	Disease status	Activity of disease	Age	Sex	SALT score	Type of AA
Patient1	Active	Severe	43	Male	80	Alopecia totalis
	Stable	Stable	43	Male	0	
Patient2	Active	Severe	30	Female	50	Patchy AA
	Stable	Stable	30	Female	20	
Patient3	Active	Severe	44	Female	90	Acute Diffuse and Total alopecia
	Stable	Stable	44	Female	0	
Patient4	Active	Severe	26	Female	60	Patchy AA
	Stable	Stable	28	Female	4	
Patient5	Active	Severe	24	Male	70	Patchy AA
	Stable	Stable	26	Male	0	

AA, alopecia areata; SALT, severity of alopecia tool

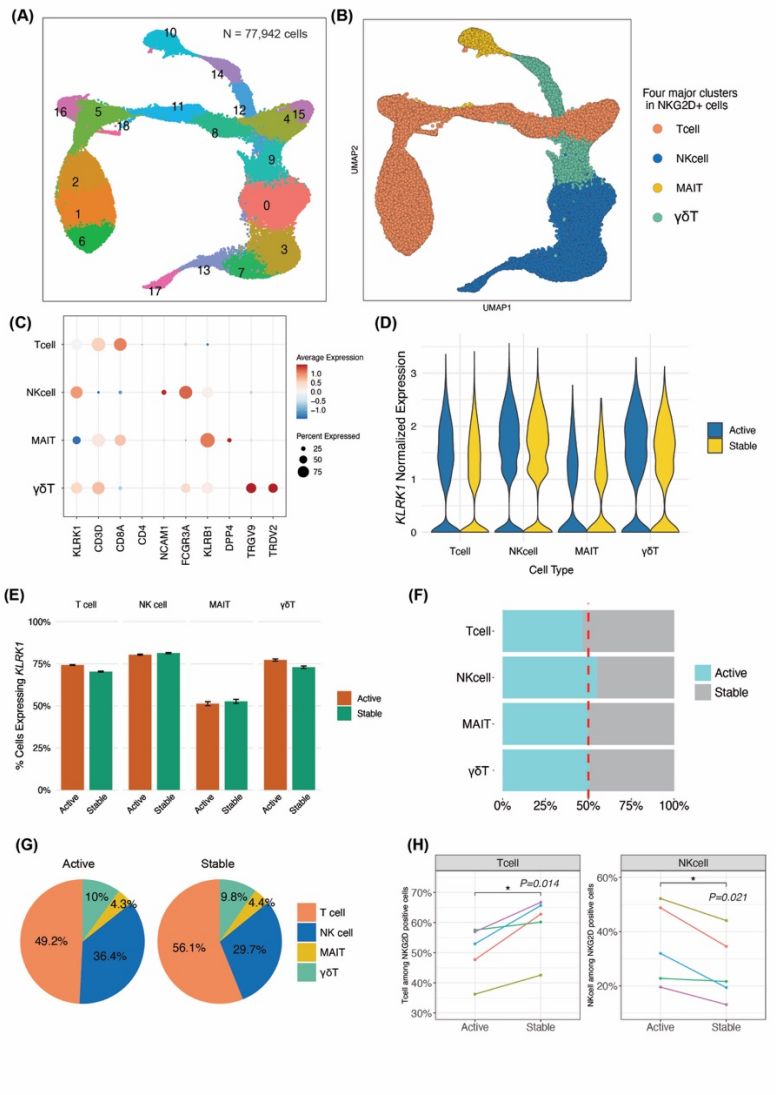

Figure 3. Analysis of NKG2D+ sorted blood cells using scRNA-seq in four major cell types.
(A) Unsupervised UMAPPlot including 77,942 cells. (B) Four major cell types (T cells, NK cells, γδT and MAIT cells) were included in the NKG2D sorted cells (C) DotPlot showing representative genes for each cell clusters. (D) *KLRK1*(= NKG2D) expression in four cell types. (E) Percentage of KLRK1 expressing cells. (F) Proportional plot showing difference of cell proportion between the active and stable status. T cells are decreased in active status, while NK cells are increased. (G) Pie plot of cell types showing difference between active and stable status (H) Paired t-test analysis of 5 paired samples of T and NK cells among NKG2D+ cells show statistically meaningful differences. Significance is shown in comparison observed by using paired t test. (*p< 0.05)

3.4. Flow Cytometry Evaluation of NKG2D+ cells

To validate the cell composition observed in our single-cell RNA sequencing (scRNA-seq) dataset, I performed flow cytometry analysis on NKG2D+ cells from patients with active and stable disease status. A total of 7 patient samples were included as pairs (Table 3). Flow cytometry evaluation on the general proportion of lymphoid cells did not show changes in CD8, NK, MAIT cells and γδT cells (Figure 4A). To confirm the trend seen in the scRNA-seq data, I evaluated NKG2D+ cell proportion among total NKG2D+ cells. Decreased proportion of NKG2D+ CD8 T cells and an increased proportion of NKG2D+ NK cells were identified in the active disease state compatible with scRNA-seq results (Figure 4B). As identified in the scRNA-seq dataset, MAIT cells and γδT cells did not show difference between status. These results suggest that the expansion of NK cells and the reduction of CD8 T cells are characteristic features of NKG2D+ cell dynamics in the active phase of AA, as suggested in the scRNA-seq dataset.

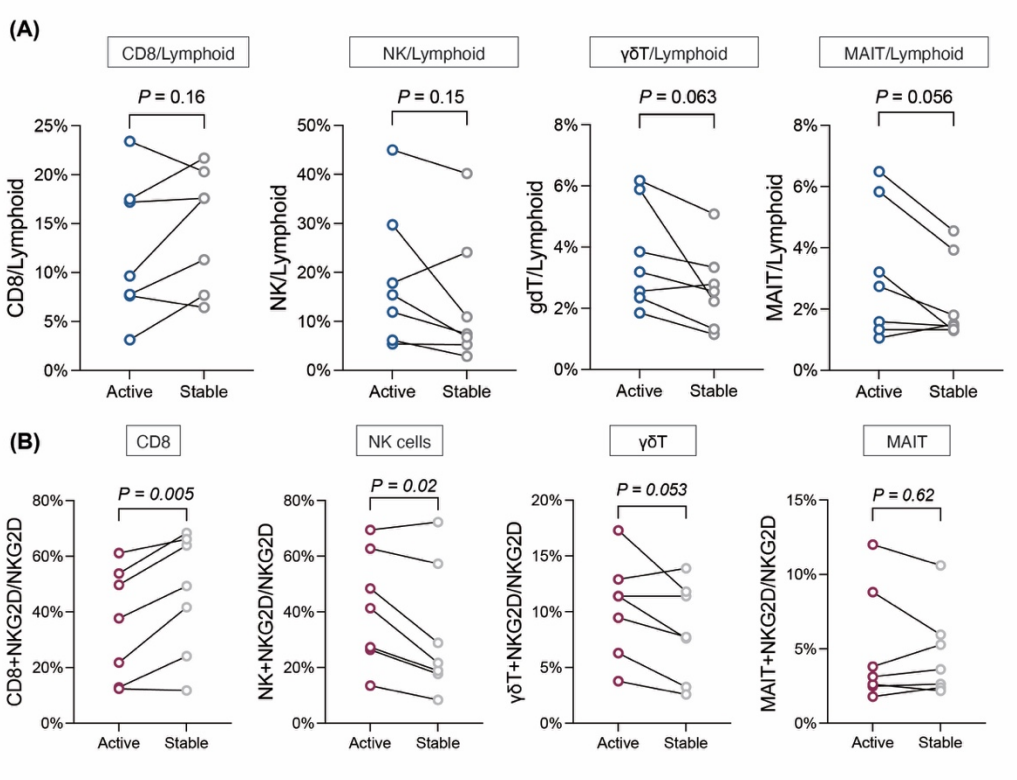

Figure 4. Flow cytometry analysis evaluation confirms cell composition change cell proportions of NKG2D+ cells. (n=7 samples in pair) (A) Proportion of each cell type among general lymphoid cells. NK cell, γδT and MAIT cells are increased in proportion among lymphoid cells while CD8 is slightly decreased in the active status. No statistical differences were identified. (B) NKG2D+ CD8 T cells show a decreased proportion among total NKG2D+ cells in the active state of AA. NKG2D+ NK cells show an increased proportion among total NKG2D+ cells in the active state of AA. The NKG2D+ γδT, MAIT cells do not show difference between active and stable status of AA. Significance is shown in comparison observed by using paired t test. (*p< 0.05)

Table 3. Patient information included in the flow cytometry analysis of paired samples

Patient	Disease status	Activity of disease	Age	Sex	SALT score
Patient1	Active	Severe	19	Female	85
	Stable	Stable	20	Female	10
Patient2	Active	Mild	43	Female	30
	Stable	Stable	43	Female	5
Patient3	Active	Severe	22	Male	100
	Stable	Mild	22	Male	5
Patient4	Active	Severe	23	Male	100
	Stable	Stable	23	Male	4
Patient5	Active	Severe	45	Male	20
	Stable	Stable	45	Male	0
Patient6	Active	Mild	40	Female	80
	Stable	Stable	42	Female	0
Patient7	Active	Mild	24	Female	30
	Stable	Stable	24	Female	0

SALT, severity of alopecia tool

3.5. Composition of detailed NKG2D + cell changes

After evaluating the general composition of the main cell subtypes of NKG2D-positive cells, I annotated each cell clusters in higher resolution. A total of 10 cell types were annotated (Figure 5A). T cells subclustered into 5 cell types including central memory T cells (Tcm), effector memory T cells (Tem), activated T cells, GATA3+ CD8 T cells and cytotoxic T lymphocytes (CTL) (Figure 5B). NK cells were subclustered into 3 cell types including CD56bright, CD56 dim and Adaptive NK(NKG2C+) cells (Figure 5B). MAIT cells and γδT cells could not be subclustered due to low proportion in cell number. Evaluation of the cell clusters in high resolution suggested that all cell types of NK cells were increased in the active status (Figure 5C). On the other hand, though the overall number of T cells were decreased in previous analysis, specific clusters with 'higher cytotoxicity' and differentiated cytotoxic T lymphocytes were increased in the active status, with decreased proportion in Naïve and Tcm cells (Figure 5C,D). This suggests that cytotoxic T lymphocytes are expanded or differentiated from other cell types. Though the NK cells are increased, I further focused on the CD8 T cells since the tissue infiltration of alopecia areata is predominantly CD8 T cells, and NK cells are inhibited by MHC molecules which hair follicles express at an inflammatory status. Given the established role of CD8 in AA pathogenesis, understanding the functional and proportional changes in cytotoxic CD8 T cells provides deeper insights into disease activity and potential therapeutic targets.

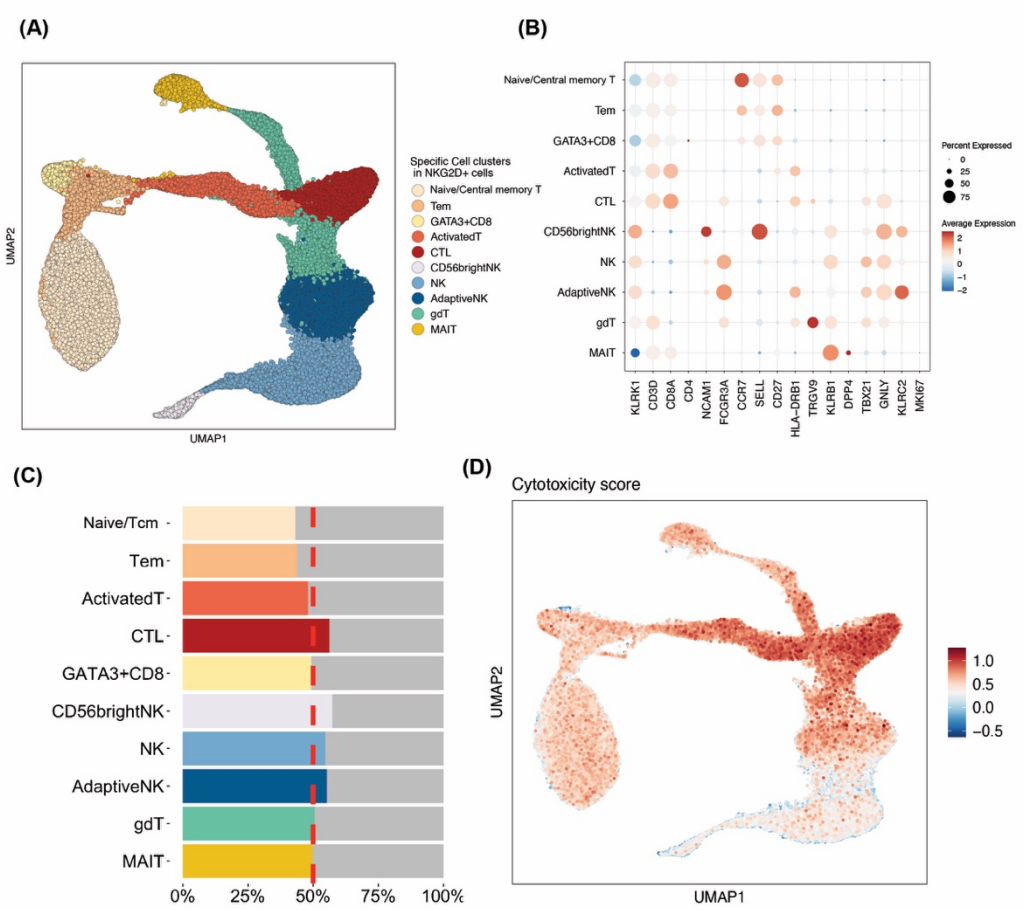

Figure 5. Analysis of NKG2D+ cells subsets in scRNA-seq by annotating different types of T cells and NK cells. (A) Annotation in higher resolution to evaluate specific cell subsets. T cells were subclustered into five clusters, NK cells into three clusters. (B) DotPlot of representative genes of all cell types. (C) Proportional plot showing difference of cell proportion between the active and stable status. Cytotoxic T lymphocytes are increased among the decreased portion of T cells. (D) Cytotoxicity gene module scoring analysis shows that cytotoxic T lymphocytes have higher cytotoxicity compared to naïve, central memory T cells.

3.6. Subset analysis of NKG2D+CD8 T cells

To focus and identify the specific changes in CD8 T cells, I subsetted CD8 T cells for further analysis. Among cells which were annotated as CD8 T cells, only the cells which were positive of T cell receptors (TCR) were included for further analysis (n= 38,262 cells) (Figure 6A). Subsetted T cells were annotated into 7 types of T cells using cell specific markers. (Figure 6B, C). T cells were clustered based on the cytotoxicity and differentiation. (Figure 6D). Proportional cell changes showed increase in cytotoxic and activated T lymphocytes including GZMB+, GZMK+, HLA-DR+ CD8 T cells (Figure 6E).

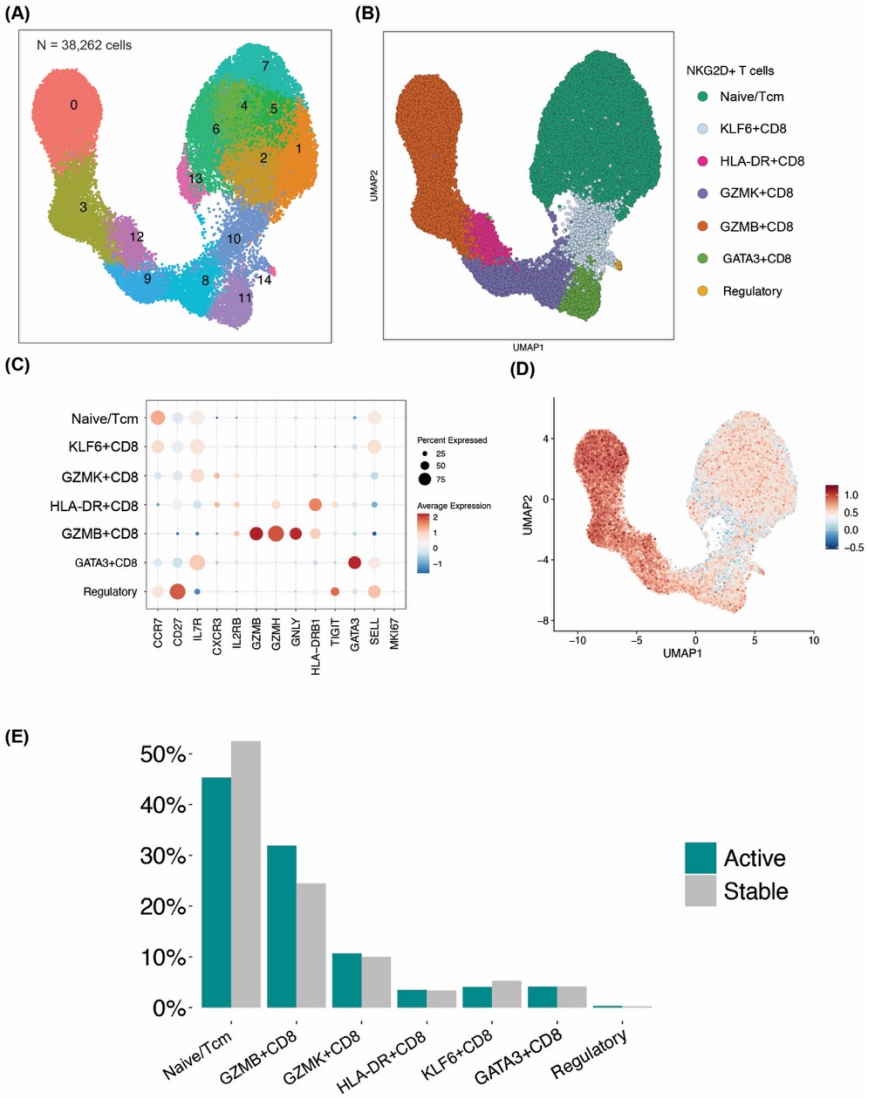

Figure 6. Subset analysis of NKG2D+ T cells. (A) Unsupervised UMAPPlot including 38,262 NKG2D+ T cells. (B) T cell subtypes differentiated by markers using unsupervised clustering. Total of 7 types of T cells were annotated. (C) DotPlot of representative genes of specific T cell subtypes. (D) Cytotoxicity gene module score using module score of cytotoxicity related genes in the T cell dataset. Cell clusters are dependent on the cytotoxicity and differentiation of CD8 T cells. (E) Proportional plot showing difference of cell proportion between the active and stable status show increase in GZMK+, GZMB+, HLA-DR+ CD8 T cells.

3.7. Differential abundance analysis of NKG2D+ CD8 T cells

To assess the changes in the abundance of NKG2D+ CD8 T cell populations in an unbiased manner, I performed a differential abundance analysis using the MILO package. (Figure 7A). This approach allows for neighborhood-based differential testing, enabling the detection of changes in cellular composition across conditions. Seurat-derived cluster annotations were incorporated into the MILO dataset metadata to aid in interpretation.

The results revealed a significant increase in the proportion of GZMB+, GZMK+, HLA-DR+ CD8 T cells in the active status of AA compared to the stable condition (Figure 7A, B). These findings suggest an enrichment of cytotoxic CD8 T cells expressing granzyme and activation markers, which may contribute to disease pathogenesis through heightened effector activity. Conversely, central memory T cells and naïve CD8 T cells showed a decrease in the active status indicating a shift away from precursor and memory subsets. (Figure 7B). Median log-fold change (logFC) values further confirmed these trends (Figure 7C). The greatest increase was observed in GZMK+ CD8 T cells, while the decreases were noted in naïve and central memory T cell clusters. These changes collectively indicate a transition towards a more differentiated and activated CD8 T cell profile in active AA.

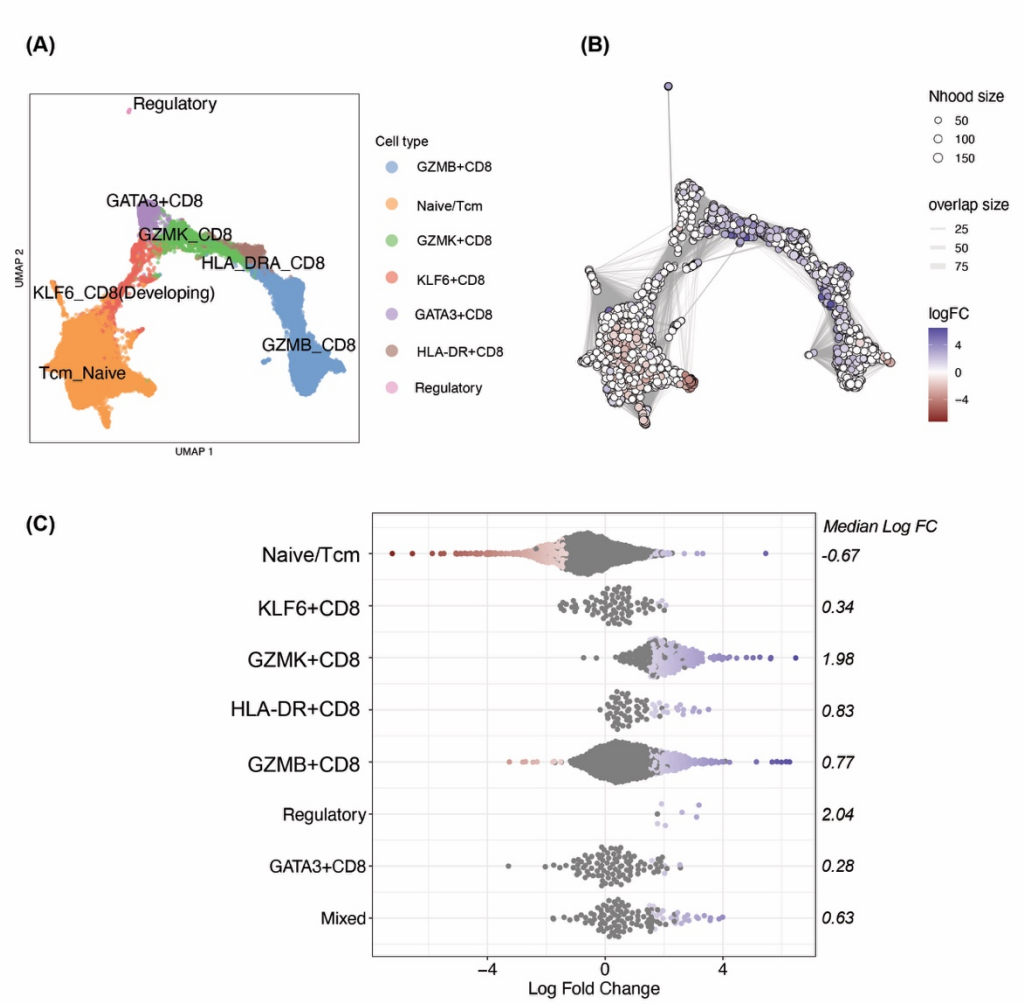

Figure 7. Differential abundance analysis of NKG2D+ T cells using MILO. (A) UMAP plot generated by the MILO package using K-Nearest Neighbors (KNN) analysis. (B) Visualization of Log-FC from differential neighborhood abundance testing. Neighborhoods with significant differential abundance are colored by log-FC (Red: negative log-FC, decreased proportion in AA; Blue: positive log-FC, increased proportion in AA). $GZMK^+$, $GZMB^+$, and $HLA\text{-}DR^+$ CD8 T cells are enriched in the active phase of AA. (C) Beeswarm plot showing the distribution of differential abundance fold changes across different cell types. GZMK + CD8 T cells show the highest median log-FC value suggesting abundance in the active status of AA. Naïve/Tcm are decreased in proportion suggesting an immunologic shift.

3.8. Flow Cytometry analysis of CD8 T cells

To confirm changes in the proportions of CD8+ T cell subtypes, I evaluated GZMB, GZMK, and HLA-DR expression using flow cytometry across 7 paired samples (Table 3). Among the CD8+ T cells, GZMK+ CD8+ T cells were increased in the active disease status, while GZMB+, HLA-DR+ CD8 T cells did not show statistical difference (Figure 8A). Next, I analyzed CD8 T cell composition and GZMK expression using CCR7 and CD45RO markers to classify CD8 T cell subsets. In the stable state, naïve CD8+ T cells (CCR7+, CD45RO-) were increased, followed by central memory T cells (Tcm; CCR7+, CD45RO+). In contrast, effector memory T cells (Tem; CCR7-, CD45RO+) and Temra cells (Temra; CCR7-, CD45RO-) were more prevalent in the active state (Figure 8B), although these differences were not statistically significant. Additionally, GZMK expression in all each 4 types of CD8+ T cell subsets did not show significant differences between active and stable statuses (Figure 8C). By combining the results of changes in CD8 T cell composition and GZMK expression, I identified that GZMK+ CD8+ Temra cells were increased in the active disease state (Figure 8D). Although not statistically significant, increase in GZMK+ Tem cells(p=0.056) was also observed in the active state (Figure 8D). These findings suggest that GZMK expression can be used as a marker of active disease status in AA, aligning with observations from the scRNA-seq dataset.

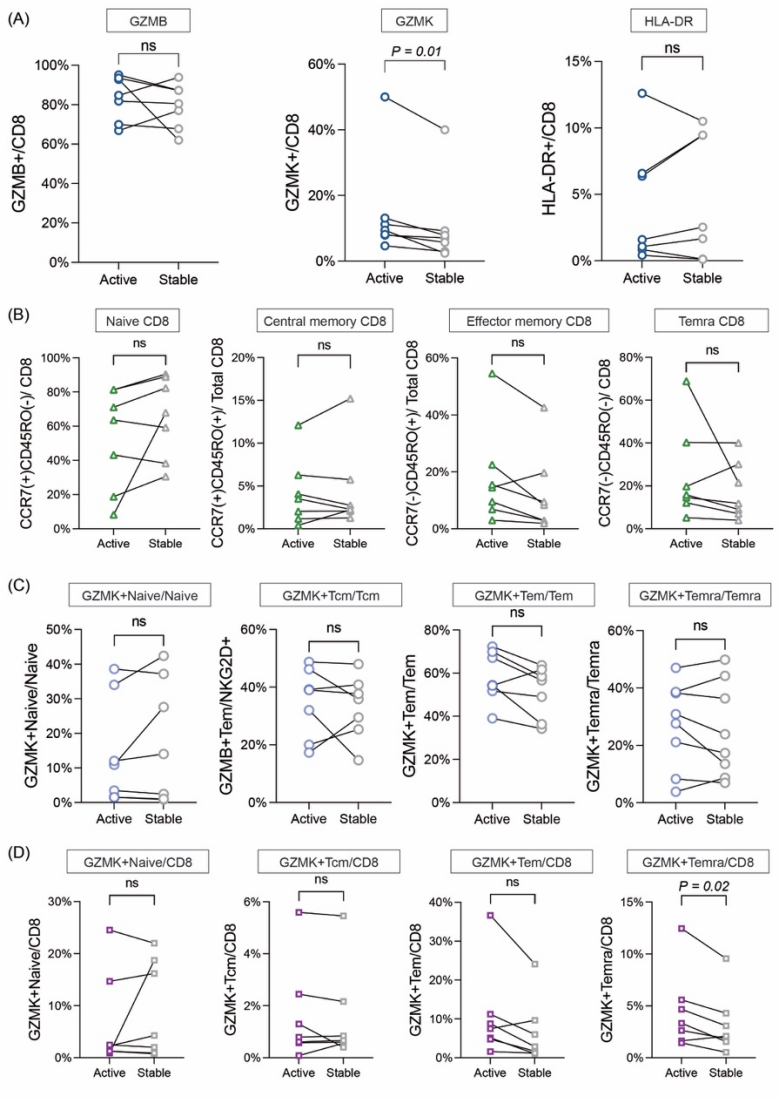

Figure 8. Flow cytometry analysis on CD8 T cells. (A) Evaluation of GZMB, GZMK, HLA-DR expression in CD8 T cells. Selected markers were identified from the scRNA-seq dataset. (B) Composition of $CD8^+$ T cell subsets based on CCR7 and CD45RO expression (naïve CD8+ T cells (CCR7+, CD45RO-), central memory T cells (Tcm; CCR7+, CD45RO+), effector memory T cells (Tem; CCR7-, CD45RO+) and Temra cells (Temra; CCR7-, CD45RO-)). (C) GZMK expression among each CD8 T cell types do not show differences between active and stable status. (D) GZMK+ cell proportion among CD8 T cells show increase of GZMK+ Temra cells in the active status of AA.

3.9. Pathway analysis of differential expressed gene in total T cells reveal upregulated cytotoxicity and activation of T cells

To investigate the molecular factors underlying immunologic shifts in NKG2D+ CD8 T cells, I first identified differentially expressed genes (DEGs) between the 'active' and 'stable' disease states. Differential expression analysis was performed, using FindMarkers function and genes were considered significantly upregulated if they met the criteria of adjusted *p*-value < 0.05 and log2 fold change (Log2FC) > 0.5. A total of 290 upregulated genes in the active status of AA (Figure 9A). To further explore the biological significance of these upregulated genes, I conducted a pathway enrichment analysis using the Metascape. The analysis revealed enriched pathways associated with T cell activation and immune regulation. Notably, pathways such as 'T cell activation', 'Regulation of leukocyte cytotoxicity', and 'Adaptive immune response' were significantly upregulated in the active disease state (Figure 9B). These findings suggest that CD8 T cells in the active phase of AA exhibit enhanced activation and increased cytotoxicity potential.

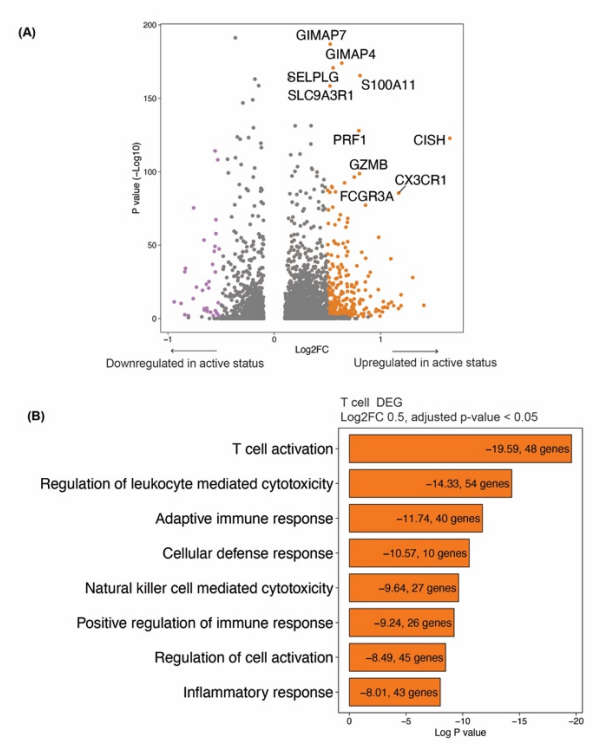

Figure 9. Transcriptome changes and pathway analysis of T Cells. (A)VolcanoPlot of differentially expressed genes in total T cells. In the active status, T cells show up-regulated genes including cytotoxicity related genes and activation signals. (B) Pathway analysis using Metascape reveals a shift in the T cell transcriptome towards an activated and cytotoxic phenotype.

3.10. Upstream analysis to identify the change in T cells

To identify the causable factor that has affected the immunologic shift among NKG2D+ CD8 T cells showing increased proportion of cytotoxicity, I evaluated the upstream signals that can cause transcriptomic changes in T cells. Evaluation of upstream signals which lead to the modification of T cell transcriptome was done using ingenuity pathway analysis (IPA). Results revealed that cytokine signals including IL-15, IFN-a, and IL-12 can be the causes for the immunologic shift in T cells (Figure 10). Among these, IL-15 showed the highest Z-score, suggesting it may be the most influential factor promoting the activation and cytotoxic programming of $CD8^+$ T cells in the active state of AA.

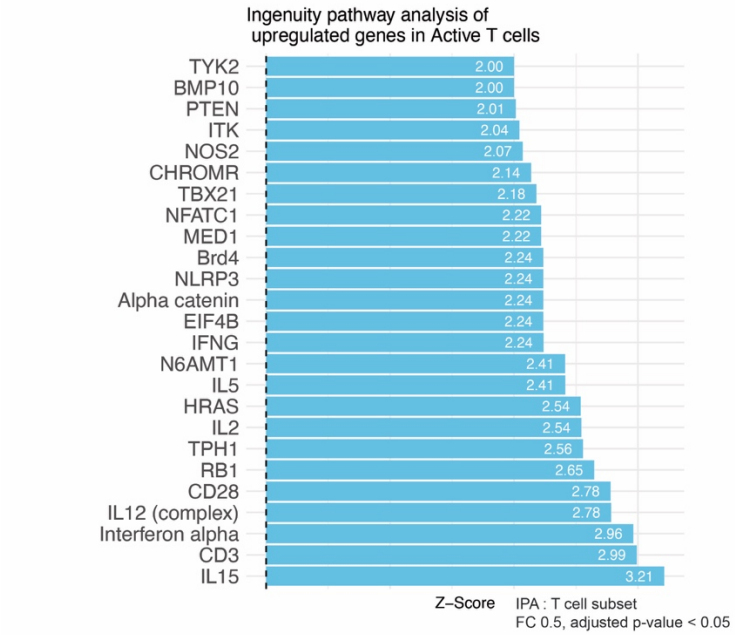

Figure 10. Upstream ingenuity pathway analysis shows causable factors that cause transcriptomic changes in NKG2D+ T cells. Cytokine Signals including IL-15, IFN-alpha, and IL-12 can be the causes for the immunologic shift in T cells. IL-15 had the highest Z-score, indicating its strong association with enhanced cytotoxic and activation-related gene expression in the active phase of AA.

3.11. Interleukin 15 down signaling is increased in the active status of T cells

To assess IL-15 signaling in NKG2D+ CD8 T cells, I performed Gene Set Enrichment Analysis (GSEA) using differentially expressed genes (DEGs). GSEA identifies whether a predefined gene set is significantly enriched in a specific condition. To evaluate IL-15 signals, I analyzed IL-15 signaling from the REACTOME database, including key signaling components such as *IL15RA*, *JAK1*, and *JAK3*. The results showed a normalized enrichment score (NES) of 2.5 with an adjusted *p*-value of 0.005, indicating that IL-15 downstream signaling is significantly increased in active T cells (Figure 11).

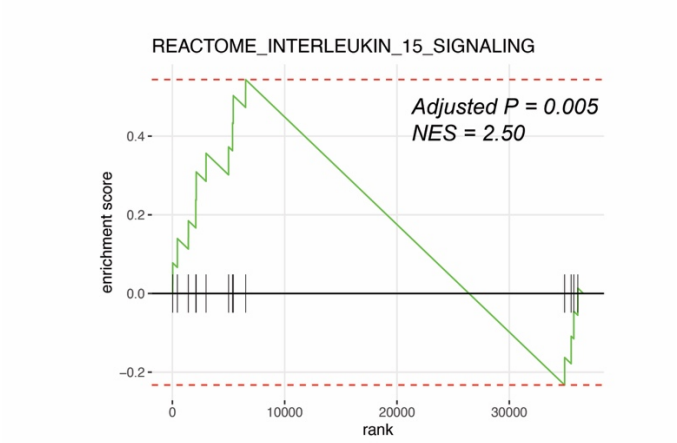

Figure 11. Gene Set Enrichment Analysis (GSEA) analysis of differentially expressed gene in T cells. GSEA using REACTOME pathway genes revealed enhanced IL-15 downstream signaling in the transcriptome of NKG2D^{+} CD8^{+} T cells during the active disease state. NES; normalized enrichment score.

3.12. Interleukin 15 level does not show differences between the active and stable status of AA

Since IL-15 has been identified as a key factor influencing T cell transcriptomic changes, I evaluated its levels in blood plasma. Firstly, I compared IL-15 between AA patients and healthy control. IL-15 concentrations were increased in AA patients (Table 4, Figure 12A). When comparing the 'active' and 'stable' states in paired samples, IL-15 concentrations were measured via ELISA in 16 patient samples, with four samples falling out of the detection range. In the remaining 12 samples, IL-15 levels were 293.2 pg/mL (SD: 427.7) in the active state and 303.5 pg/mL (SD: 311.0) in the stable state (Table 4). Level of IL-15 varied considerably between individuals, and no statistically significant difference was observed between disease states (Figure 12B). These findings suggest that cytokine levels can depend on interpersonal variation. Also, IL-15 alone may not serve as a reliable marker for disease activity in AA.

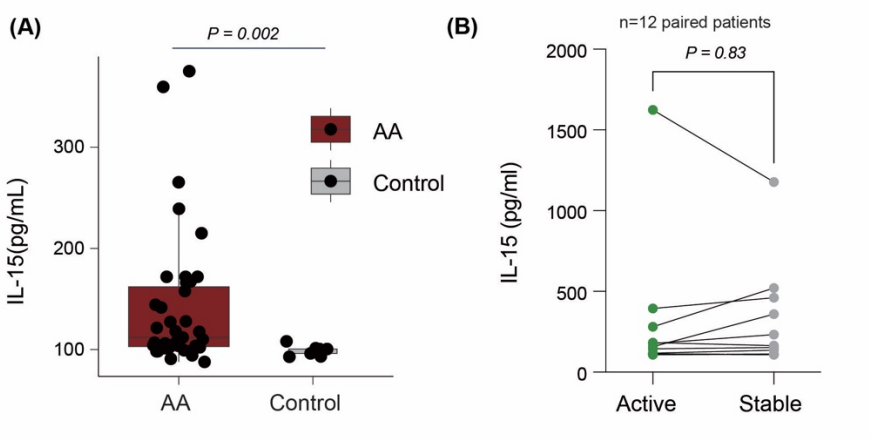

Figure 12. Serologic evaluation of cytokine level changes using ELISA. (A)Plasma IL-15 concentrations were increased in AA patients compared to healthy control. (B) Paired samples did not show significant difference between active and stable states, with levels being more dependent on individual patient variability.

Table 4. Patient information included in the paired evaluation on IL-15 with ELISA.

Patient	Group	Activity of disease	Age	Sex	SALT score
Patient1	Active	Severe	23	Male	100
	Stable	Stable	23	Male	4
Patient2	Active	Severe	45	Male	20
	Stable	Stable	45	Male	0
Patient3	Active	Severe	19	Female	85
	Stable	Stable	20	Female	10
Patient4	Active	Mild	24	Female	30
	Stable	Stable	24	Female	0
Patient5	Active	Severe	50	Female	38
	Stable	Stable	51	Female	0
Patient6	Active	Severe	61	Female	100
	Stable	Stable	61	Female	0
Patient7	Active	Mild	43	Female	30
	Stable	Stable	43	Female	5
Patient8	Active	Severe	44	Female	100
	Stable	Mild	44	Female	30
Patient9	Active	Severe	43	Male	80
	Stable	Stable	43	Male	0
Patient10	Active	Severe	44	Female	90
	Stable	Stable	44	Female	0
Patient11	Active	Severe	26	Female	60
	Stable	Stable	28	Female	4
Patient12	Active	Severe	24	Male	70
	Stable	Stable	26	Male	0

SALT, severity of alopecia tool

3.13. Bulk RNA sequencing of Innate Immune Cells Does Not Reveal Changes in cytokine Expression

To identify further evaluation of innate immune cells which are potential producers of cytokines and since IL-15 exists in both soluble and membrane-bound forms, I evaluated its expression at the transcriptomic level. HLA-DR+ CD14+ monocytes were sorted from three paired patient samples, and bulk RNA sequencing was performed to investigate gene expression changes (Table 5, Figure 13A). Differentially expressed genes were achieved comparing the active and stable status (Figure 13B). *IL15* showed a mild increase in the active state (log2FC = 0.06); however, the adjusted p-value (p = 0.096) was not statistically significant. Pathway analysis was done using DEGs with significance threshold of $p < 0.05$ and log2FC > 0.5, and I identified 205 differentially expressed genes (DEGs) (Figure 13C). No signatures related to cytokine production was identified. These findings suggest that monocytes do not exhibit significant changes in cytokine expression including IL-15 at the transcriptomic level.

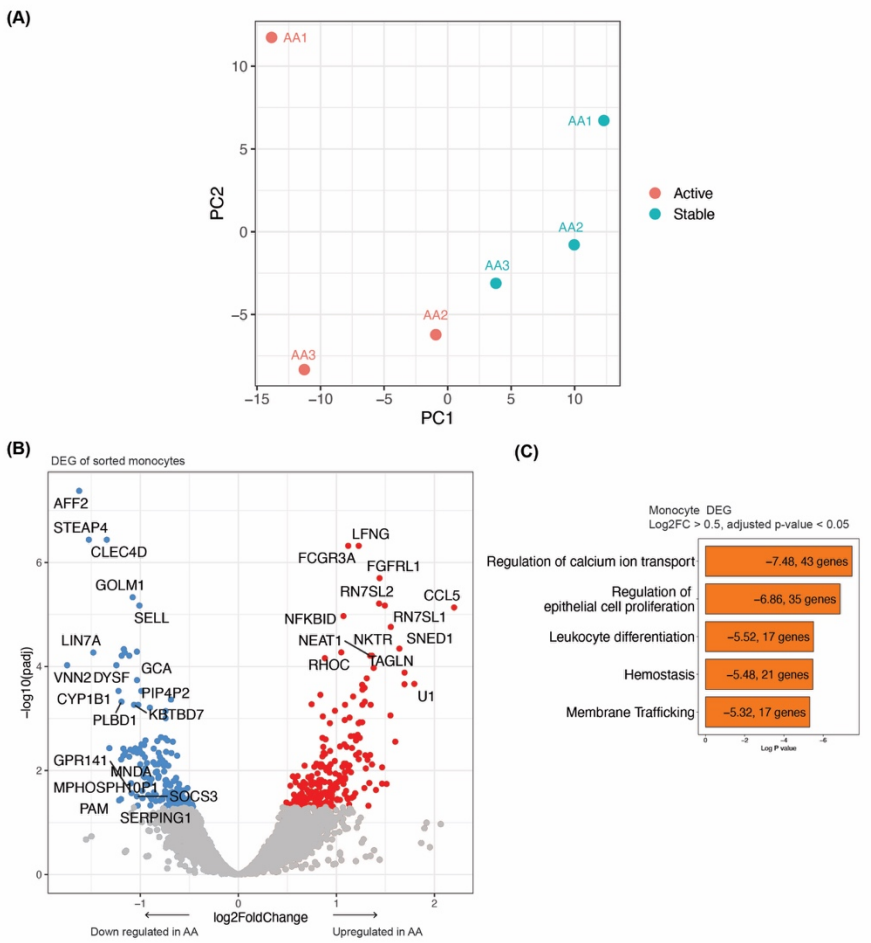

Figure 13. Transcriptomic evaluation of monocytes using bulk RNA sequencing to assess cytokine expression changes. (A) Principal component analysis (PCA) of three paired samples (active vs. stable). (B) Volcano plot of differentially expressed genes between active and stable states. *IL15* is not identified as a significantly differentially expressed gene. (C) Pathway analysis of monocyte DEGs using Metascape reveal no pathways related to cytokine production.

Table 5. Patient information included in the bulk RNA seq analysis of monocyte sorted cells.

Patient	Group	Activity of disease	Age	Sex	SALT score
Patient1	Active	Mild	24	Female	30
	Stable	Stable	24	Female	0
Patient2	Active	Severe	50	Female	38
	Stable	Stable	51	Female	0
Patient3	Active	Severe	61	Female	100
	Stable	Stable	61	Female	0

4. DISCUSSION

This study aimed to identify the immunologic changes in the blood of alopecia areata patients to uncover the systemic changes between the status of disease. Since recent studies has shown the increased risk of alopecia areata due to systemic factors (e.g. COVID vaccination and seasonal allergies) and the correlation in inflammatory signals between blood and skin, alopecia areata can be suggested as a more than a skin specific disease. [34, 35]

Though previous studies focused on identifying the NKG2D+ cells in AA patient blood, most studies focused on the comparison between AA patients and healthy control, which cannot associate with clinical characteristics of AA. [17, 28] Our study focused on identifying the correlation between NKG2D cells and the clinical characteristics including activity and severity. Also, since NKG2D, which is expressed in ~100% of human cytotoxic cells in contrast to murine, demand for uncovering further markers more than NKG2D was required. Therefore, this study focused on NKG2D+ cells at the systemic levels using scRNA-seq analysis.

In our basic analysis, we found that the frequency of NKG2D-expressing lymphoid cells was not significantly different between AA patients and healthy controls. However, NKG2D levels in NK cells (CD3-, CD56+) and CD3+CD56+ cells were increased in AA patients, similar to previous findings. [28] Differences in CD4 and CD8 T cells compared to prior studies may be due to variations in statistical methods, as previous studies relied on fold-change values, whereas our approach focused on population proportions. When stratifying AA patients by disease severity and activity, no correlation was observed between severity and NKG2D+ cell proportions. However, disease activity was inversely correlated with NKG2D+ CD8 T cell proportions, whereas NKG2D+ NK cells increased in active disease, though these associations were not statistically significant.

The change in blood immune status seemed to correlate with activity rather than severity. This is similar to some previous studies which tried to identify markers with correlation to disease activity. [36] However, most studies focused on the comparison between AA patients and healthy controls for the discovery of potential biomarkers. [23, 24] Though severity is not a contrary factor to activity, evaluating immune status with disease activity seems to be more plausible since hair loss is caused ‘after’ the attack of hair follicles leading to a hair cycle change into acute telogen or catagen. [37] Also, use of hair pull test or trichoscopy findings rather than SALT score to evaluate activity supports the gap between activity and severity. [38, 39]

To further elucidate disease activity related immune changes and minimize inter-individual variability, a ‘paired’ set of analysis on individual patients was done, comparing the active and stable status. Therefore, I sorted NKG2D+ cells from ‘active’ and ‘stable’ status of AA and analyzed with scRNA-seq to enable an unbiased evaluation of cellular composition and transcriptional changes.

The scRNA-seq dataset generated from sorted NKG2D+ cells included CD8 T cells, NK cells, mucosal-associated invariant T (MAIT) cells, and γδ T cells, all of which are known for their cytotoxic properties. This is compatible with facts that the 4 types of cells express NKG2D in most of the cells in human. [15] Among the cell subtypes, disease activity and NKG2D+ CD8 T cells show an inverse correlation. NKG2D+ NK cells on the other hand are increased in the active status. This may have been due to the result that NK cells express more NKG2D in the active status, possibly

caused by an IL-15 increase, resulting in increased number of selections during the NKG2D-positive cell sorting process. Consequently, the proportion of CD8 T cells, which are the primary proportion of NKG2D+ sorted cells may have been affected due to the increased selection of NKG2D+ NK cells, leading to a decrease in proportion.

Among the decreased proportion of NKG2D+ CD8 T cells, interestingly, cytotoxic and activated CD8 T cells (GZMK, GZMB, HLA-DR+) were found to be expanded in the active phase, as revealed by the scRNA-seq dataset. This was confirmed in the unsupervised differential abundance analysis using MILO.[31] In the analysis, GZMK+ CD8 T cells was the most increased cluster with the highest median value. On the other hand, central memory T or naïve T cells were decreased in proportion. Regarding the proportional shift of T cells, it can be suggested that the naïve, central memory T cells were activated, leading to differentiation and expansion of cytotoxic T cells. The shift in immune cell composition may have been due to the activation of T cells leading to increased cytotoxicity and adaptive immune responses which are confirmed by the pathway analysis of differentially expressed genes obtained from T cells.

Flow cytometry analysis aligns with the scRNA-seq dataset showing an increase in GZMK+ CD8 T cells, particularly the GZMK+CCR7-CD45RO- subset, during the active status of AA. This aligns with previous findings showing that CD8+ effector T cells re-expressing CD45RA(Temra) are elevated in intractable AA and infiltrate skin tissue.[40] Additionally, earlier studies have demonstrated that GZMK+ CD8 T cells are present in the skin of AA patients, supporting the plausibility of their increase in human PBMCs during the active phase.[41, 42] Also, given that GZMK expression is primarily driven by cytokine signaling rather than TCR activation, this underscores the role of cytokine-induced immune shifts in AA pathogenesis.[43] Since the scRNA-seq dataset could not differentiate Tem and Temra due to limitation in using CD45RA, CD45RO as markers, further studies are required.

To identify the specific cause of the immunologic shift, I focused on identifying the factors that led to the change in T cells. Since many factors can induce the activation and differentiation in T cells, I only selected samples that was not affected by known factors such as viral infections nor cancer. If a patient showed any symptoms suspecting viral signs, the sample was not included in the study. All patients were not diagnosed as cancer and did not have any history of malignancy.

Upstream signaling analysis using the transcriptomic changes was done to assess the causable factors. Ingenuity pathway analysis (IPA) implicated cytokines such as *IL-15, IL-12,* and *IFN-α,* along with T cell receptor (TCR) activation as main factors. However, since specific TCRs nor antigens have been identified in AA, I focused on cytokine-driven immune alterations.

Since IL-15 was the main upstream signal and confirmed that the downstream signals were shifted in T cells by GSEA, cytokine-induced T cell activation was suspected. Recently the concept of virtual memory T cells, which can be activated by cytokines emerged as an important pathogenesis in AA animal models.[44] Though I could not prove the presence of virtual memory T cells due to the poorly identified marker in human and the limitation that it could not be identified as a specific cluster in the scRNA-seq dataset, the concept of ‘cytokine’ activation has similar properties. Also, considering that NKG2D levels are increased with exposure to IL-15, the cytokine was considered a promising cytokine.[15]

As in previous studies, AA patients showed higher IL-15 levels compared to healthy control. [45, 46] However, within the paired samples, cytokine levels did not show increase in the active status. Within the experiment, cytokine levels of four patients were undetectable in both active and stable states due to excessively high values. This suggests that inter-individual variability may outweigh disease status as a determinant of IL-15 expression in blood, potentially limiting its sensitivity as activity biomarker for AA. Regarding that IL-15 may be the cause of immunologic shifting but is not identified in blood, the source of the possible cytokine needs further research (e.g. scalp).

Our results suggest that AA involves systemic immune alterations beyond the skin, with a shift toward an effector phenotype in CD8 T cells in the active status of AA. Increased cytotoxic T cell (GZMK+) and a reduction in naïve and central memory subsets highlight potential biomarkers for disease activity and therapeutic targets. Also, increased NK cell proportion among NKG2D+ cells were identified.

This study has several strengths, including being the first to analyze blood cells with a specific focus on NKG2D. Additionally, the correlation with disease activity in paired samples reinforces the immunologic role of NKG2D in AA. Our findings have clinical relevance for patients with AA, a disease with an unpredictable course. The observed immunologic shift and increase in GZMK+ T cells may serve as potential disease markers, guiding treatment decisions based on disease activity. If blood analysis can identify active disease status, proactive treatment may facilitate earlier immune stabilization, potentially preventing the development of new alopecic patches. Since hair regrowth in alopecic patches requires a prolonged period, prevention is crucial. This approach may improve patients' quality of life and alleviate the frustration caused by unpredictable hair loss.

This study has several limitations. The analysis did not include all cell types of PBMC immune subsets, and proportional changes could be influenced by NKG2D expression dynamics rather than true population shifts. Additionally, possible factors driving these 'immune shift' remain unclear. Future studies should aim to correlate scalp inflammation with systemic immune profiles, as direct tissue analysis may provide more definitive insights into disease pathogenesis despite challenges in obtaining patient samples.

5. CONCLUSION

Our findings highlight a systemic shift in immune composition during active AA, characterized by an enrichment of highly cytotoxic T cells and NK cells. This shift suggests that AA is not merely a localized skin disorder rather a disease involving system-wide alterations in immune regulation. The expansion of GZMB+ and GZMK+ CD8 T cells in active disease underscores the role of cytotoxic T cell responses in disease activity. While IL-15-driven immune alterations remain a potential mechanistic link, its variability across individuals limits its use as a biomarker. Nonetheless, our study suggests that cytotoxic T cell enrichment could serve as a more robust biomarker for disease activity and potentially guide therapeutic interventions. Future studies integrating peripheral and lesional immune profiles correlating with disease activity may further refine our understanding of immune dysregulation in AA and uncover new targets for treatment.

Table 6. Clinical information of patients included in the study.

	Status	Age	Sex	Activity	SALT	Type of AA	Experiments
Patient 1	Active	27	M	1	30	Patchy AA	Flow cytometry (vs HC)
Patient 2	Active	28	M	1	20	Patchy AA	Flow cytometry (vs HC)
Patient 3	Active	18	M	1	10	Patchy AA	Flow cytometry (vs HC)
Patient 4	Active	25	M	1	20	Patchy AA	Flow cytometry (vs HC)
Patient 5	Active	25	M	1	40	Patchy AA	Flow cytometry (vs HC)
Patient 6	Active	23	M	1	80	Alopecia Totalis	Flow cytometry (vs HC)
Patient 7	Active	23	F	1	75	Alopecia Totalis	Flow cytometry (vs HC)
Patient 8	Active	58	F	1	25	Patchy AA	Flow cytometry (vs HC)
Patient 9	Active	62	M	Mild	100	Alopecia Universalis	Flow cytometry (vs HC), IL-15 ELISA (vs HC)
Patient 10	Active	53	F	Sever	87.5	Alopecia Totalis	Flow cytometry (vs HC), IL-15 ELISA (vs HC)
Patient 11	Active	44	F	Mild	100	Alopecia Universalis	Flow cytometry (vs HC), IL-15 ELISA (vs HC), IL-15 ELISA (Paired)
	Stable	44	F	Mild	30		
Patient 12	Active	30	F	Severe	50	Patchy AA	Flow cytometry (vs HC), IL-15 ELISA (vs HC), IL-15 ELISA (Paired), scRNA-seq
	Stable	30	F	Stable	20		
Patient 13	Stable	52	F	Stable	3	Patchy AA	Flow cytometry (vs HC), IL-15 ELISA (vs HC)
Patient 14	Active	45	F	Mild	3	Ophiasis	Flow cytometry (vs HC), IL-15 ELISA (vs HC)
Patient 15	Active	30	F	Severe	100	Acute Diffuse Total alopecia	Flow cytometry (vs HC), IL-15 ELISA (vs HC)
Patient 16	Stable	47	M	Stable	25	Patchy AA	Flow cytometry (vs HC), IL-15 ELISA (vs HC)
Patient 17	Active	43	M	Severe	8	Patchy AA	Flow cytometry (vs HC), scRNA-seq, IL-15 ELISA (Paired)
	Stable	43	M	Stable	0		
Patient 18	Active	47	M	Mild	25	Patchy AA	Flow cytometry (vs HC), IL-15 ELISA (vs HC)
Patient 19	Active	44	F	Severe	100	Alopecia Universalis	Flow cytometry (vs HC), IL-15 ELISA (vs HC)
Patient 20	Active	44	F	Severe	90	Alopecia Universalis	Flow cytometry (vs HC), scRNA-seq, IL-15 ELISA (Paired)
	Stable	44	F	Stable	0		

Patient 21	Active	42	M	Mild	6	Patchy AA	Flow cytometry (vs HC), IL-15 ELISA (vs HC)
Patient 22	Active	28	F	Stable	60	Patchy AA	Flow cytometry (vs HC), scRNA-seq, IL-15 ELISA (Paired)
	Stable	26	F	Stable	4		
Patient 23	Active	44	F	Mild	8	Patchy AA	Flow cytometry (vs HC), IL-15 ELISA (vs HC)
Patient 24	Active	29	M	Mild	97.5	Alopecia Universalis	Flow cytometry (vs HC), IL-15 ELISA (vs HC)
Patient 25	Active	43	M	Severe	20	Patchy AA	Flow cytometry (vs HC), Flow cytometry (Paired), IL-15 ELISA (Paired)
	Stable	43	M	Stable	0		
Patient 26	Active	25	F	Severe	100	Alopecia Universalis	Flow cytometry (vs HC), IL-15 ELISA (vs HC)
Patient 27	Active	29	F	Severe	98	Acute Diffuse Total alopecia	Flow cytometry (vs HC), IL-15 ELISA (vs HC)
Patient 28	Active	24	M	Severe	70	Patchy AA	Flow cytometry (vs HC), scRNA-seq, IL-15 ELISA (Paired)
	Stable	24	M	Stable	0		
Patient 29	Active	44	F	Mild	15	Patchy AA	Flow cytometry (vs HC), IL-15 ELISA (vs HC)
Patient 30	Active	47	F	Mild	30	Patchy AA	Flow cytometry (vs HC), IL-15 ELISA (vs HC)
Patient 31	Active	47	M	Mild	10	Patchy AA	Flow cytometry (vs HC), IL-15 ELISA (vs HC)
Patient 32	Active	19	M	Severe	100	Alopecia Universalis	Flow cytometry (vs HC), Flow cytometry (Paired)
	Stable	19	M	Mild	5		
Patient 33	Active	22	F	Mild	25	Patchy AA	Flow cytometry (vs HC), IL-15 ELISA (vs HC)
Patient 34	Active	45	F	Severe	19	Patchy AA	Flow cytometry (vs HC), IL-15 ELISA (vs HC)
Patient 35	Active	29	F	Severe	30	Patchy AA	Flow cytometry (vs HC), IL-15 ELISA (vs HC)
Patient 36	Stable	50	F	Stable	3	Patchy AA	Flow cytometry (vs HC), IL-15 ELISA (vs HC)
Patient 37	Active	46	F	Mild	10	Patchy AA	Flow cytometry (vs HC), IL-15 ELISA (vs HC)
Patient 38	Active	38	F	Severe	75	Patchy AA	Flow cytometry (vs HC), IL-15 ELISA (vs HC)
Patient 39	Active	36	M	Severe	90	Alopecia Totalis	Flow cytometry (vs HC), IL-15 ELISA (vs HC), IL-15 ELISA (Paired)
	Stable	36	M	Stable	0		

Patient 40	Active	22	F	Mild	25	Patchy AA	Flow cytometry (vs HC), IL-15 ELISA (vs HC)
Patient 41	Active	43	M	Severe	90	Alopecia Totalis	Flow cytometry (vs HC), IL-15 ELISA (vs HC)
Patient 42	Active	39	M	Mild	90	Alopecia Universalis	Flow cytometry (vs HC), IL-15 ELISA (vs HC)
Patient 43	Active	25	M	Severe	100	Alopecia Universalis	Flow cytometry (vs HC), IL-15 ELISA (vs HC), IL-15 ELISA (Paired)
	Stable	25	M	Mild	30		
Patient 44	Active	45	F	Severe	50	Patchy AA	Flow cytometry (vs HC), IL-15 ELISA (vs HC)
Patient 45	Active	61	F	Mild	15	Patchy AA	Flow cytometry (vs HC), IL-15 ELISA (vs HC)
Patient 46	Active	39	F	Mild	30	Ophiasis	Flow cytometry (vs HC), IL-15 ELISA (vs HC)
Patient 47	Active	39	F	Mild	30	Patchy AA	Flow cytometry (vs HC), IL-15 ELISA (vs HC)
Patient 48	Active	19	F	Severe	85	Alopecia Totalis	Flow cytometry (Paired), IL-15 ELISA (Paired)
	Stable	20	F	Stable	10		
Patient 49	Active	43	F	Mild	30	Patchy AA	Flow cytometry (Paired), IL-15 ELISA (Paired)
	Stable	43	F	Stable	5		
Patient 50	Active	23	M	Severe	100	Alopecia Totalis	Flow cytometry (Paired), IL-15 ELISA (Paired)
	Stable	23	M	Stable	4		
Patient 51	Active	40	F	Mild	80	Alopecia Totalis	Flow cytometry (Paired), IL-15 ELISA (Paired)
	Stable	42	F	Stable	0		
Patient 52	Active	24	F	Mild	30	Patchy AA	Flow cytometry (Paired), IL-15 ELISA (Paired), Monocyte Bulk RNA seq (Paired)
	Stable	24	F	Stable	0		
Patient 53	Active	50	F	Severe	38	Patchy AA	IL-15 ELISA (Paired), Monocyte Bulk RNA seq (Paired)
	Stable	51	F	Stable	0		
Patient 46	Active	61	F	Severe	100	Alopecia Totalis	IL-15 ELISA (Paired), Monocyte Bulk RNA seq (Paired)
	Stable	61	F	Stable	0		

HC, Healthy control.

References

1 Pratt CH, King LE, Jr., Messenger AG, Christiano AM, Sundberg JP. Alopecia areata. *Nat Rev Dis Primers* 2017; **3**: 17011.
2 Strazzulla LC, Wang EHC, Avila L et al. Alopecia areata: An appraisal of new treatment approaches and overview of current therapies. *J Am Acad Dermatol* 2018; **78**(1): 15-24.
3 Phan K, Sebaratnam DF. JAK inhibitors for alopecia areata: a systematic review and meta-analysis. *J Eur Acad Dermatol Venereol* 2019; **33**(5): 850-856.
4 Barker CF, Billingham RE. Analysis of local anatomic factors that influence the survival times of pure epidermal and full-thickness skin homografts in guinea pigs. *Ann Surg* 1972; **176**(5): 597-604.
5 Reynolds AJ, Lawrence C, Cserhalmi-Friedman PB, Christiano AM, Jahoda CA. Trans-gender induction of hair follicles. *Nature* 1999; **402**(6757): 33-34.
6 Bertolini M, McElwee K, Gilhar A, Bulfone-Paus S, Paus R. Hair follicle immune privilege and its collapse in alopecia areata. *Exp Dermatol* 2020; **29**(8): 703-725.
7 Rajabi F, Drake LA, Senna MM, Rezaei N. Alopecia areata: a review of disease pathogenesis. *Br J Dermatol* 2018; **179**(5): 1033-1048.
8 Petukhova L, Duvic M, Hordinsky M et al. Genome-wide association study in alopecia areata implicates both innate and adaptive immunity. *Nature* 2010; **466**(7302): 113-117.
9 Simakou T, Butcher JP, Reid S, Henriquez FL. Alopecia areata: A multifactorial autoimmune condition. *J Autoimmun* 2019; **98**: 74-85.
10 Betz RC, Petukhova L, Ripke S et al. Genome-wide meta-analysis in alopecia areata resolves HLA associations and reveals two new susceptibility loci. *Nat Commun* 2015; **6**: 5966.
11 Xing L, Dai Z, Jabbari A et al. Alopecia areata is driven by cytotoxic T lymphocytes and is reversed by JAK inhibition. *Nat Med* 2014; **20**(9): 1043-1049.
12 Divito SJ, Kupper TS. Inhibiting Janus kinases to treat alopecia areata. *Nat Med* 2014; **20**(9): 989-990.
13 Wensveen FM, Jelencic V, Polic B. NKG2D: A Master Regulator of Immune Cell Responsiveness. *Front Immunol* 2018; **9**: 441.
14 Groh V, Rhinehart R, Randolph-Habecker J, Topp MS, Riddell SR, Spies T. Costimulation of CD8alphabeta T cells by NKG2D via engagement by MIC induced on virus-infected cells. *Nat Immunol* 2001; **2**(3): 255-260.
15 Raulet DH. Roles of the NKG2D immunoreceptor and its ligands. *Nat Rev Immunol* 2003; **3**(10): 781-790.
16 Dai Z, Xing L, Cerise J et al. CXCR3 Blockade Inhibits T Cell Migration into the Skin and Prevents Development of Alopecia Areata. *J Immunol* 2016; **197**(4): 1089-1099.
17 Ito T, Ito N, Saatoff M et al. Maintenance of hair follicle immune privilege is linked to prevention of NK cell attack. *J Invest Dermatol* 2008; **128**(5): 1196-1206.
18 Gilhar A, Laufer Britva R, Keren A, Paus R. Mouse Models of Alopecia Areata: C3H/HeJ

Mice Versus the Humanized AA Mouse Model. *J Investig Dermatol Symp Proc* 2020; **20**(1): S11-S15.

19 Lee S, Lee H, Lee CH, Lee WS. Comorbidities in alopecia areata: A systematic review and meta-analysis. *J Am Acad Dermatol* 2019; **80**(2): 466-477 e416.

20 Lim SH, Ju HJ, Han JH et al. Autoimmune and Autoinflammatory Connective Tissue Disorders Following COVID-19. *JAMA Netw Open* 2023; **6**(10): e2336120.

21 Dere G, Gundogdu M. Investigation of the relationship between alopecia areata and inflammatory blood parameters. *J Cosmet Dermatol* 2021; **20**(12): 4048-4051.

22 Glickman JW, Dubin C, Dahabreh D et al. An integrated scalp and blood biomarker approach suggests the systemic nature of alopecia areata. *Allergy* 2021; **76**(10): 3053-3065.

23 Glickman JW, Dubin C, Renert-Yuval Y et al. Cross-sectional study of blood biomarkers of patients with moderate to severe alopecia areata reveals systemic immune and cardiovascular biomarker dysregulation. *J Am Acad Dermatol* 2021; **84**(2): 370-380.

24 Zaaroura H, Gilding AJ, Sibbald C. Biomarkers in alopecia Areata: A systematic review and meta-analysis. *Autoimmun Rev* 2023; **22**(7): 103339.

25 Alotaibi MA, Altaymani A, Al-Omair A, Alghamdi W. Viral-Induced Rapidly Progressive Alopecia Universalis: A Case Report and Literature Review. *Cureus* 2023; **15**(4): e37406.

26 Kutlu O, Aktas H, Imren IG, Metin A. Short-term stress-related increasing cases of alopecia areata during the COVID-19 pandemic. *J Dermatolog Treat* 2022; **33**(2): 1177.

27 Christensen RE, Jafferany M. Association between alopecia areata and COVID-19: A systematic review. *JAAD Int* 2022; **7**: 57-61.

28 Jang YH, Choi JK, Jang YH et al. Increased blood levels of NKG2D(+)CD4(+) T cells in patients with alopecia areata. *J Am Acad Dermatol* 2017; **76**(1): 151-153.

29 Butler A, Hoffman P, Smibert P, Papalexi E, Satija R. Integrating single-cell transcriptomic data across different conditions, technologies, and species. *Nat Biotechnol* 2018; **36**(5): 411-420.

30 Borcherding N, Bormann NL, Kraus G. scRepertoire: An R-based toolkit for single-cell immune receptor analysis. *F1000Res* 2020; **9**: 47.

31 Dann E, Henderson NC, Teichmann SA, Morgan MD, Marioni JC. Differential abundance testing on single-cell data using k-nearest neighbor graphs. *Nat Biotechnol* 2022; **40**(2): 245-253.

32 Zhou Y, Zhou B, Pache L et al. Metascape provides a biologist-oriented resource for the analysis of systems-level datasets. *Nat Commun* 2019; **10**(1): 1523.

33 Kramer A, Green J, Pollard J, Jr., Tugendreich S. Causal analysis approaches in Ingenuity Pathway Analysis. *Bioinformatics* 2014; **30**(4): 523-530.

34 Jung SW, Jeon JJ, Kim YH, Choe SJ, Lee S. Long-term risk of autoimmune diseases after mRNA-based SARS-CoV2 vaccination in a Korean, nationwide, population-based cohort study. *Nat Commun* 2024; **15**(1): 6181.

35 Garate D, Thang CJ, Murphy TL et al. Evaluating alopecia areata risk among patients with seasonal and food allergies: A multicenter cohort study. *Allergy* 2024; **79**(12): 3525-3528.

36 Omar NM, Ghanem BM, Abdelsalam M, Elmogy MH. Serum interleukin 15 level may

serve as a new marker for alopecia areata. *Egyptian Journal of Dermatology and Venerology* 2022; **42**(1): 34-39.

37 Olayinka JJT, Richmond JM. Immunopathogenesis of alopecia areata. *Curr Res Immunol* 2021; **2**: 7-11.

38 Waskiel-Burnat A, Rakowska A, Sikora M, Olszewska M, Rudnicka L. Alopecia areata predictive score: A new trichoscopy-based tool to predict treatment outcome in patients with patchy alopecia areata. *J Cosmet Dermatol* 2020; **19**(3): 746-751.

39 Olsen EA. Investigative guidelines for alopecia areata. *Dermatol Ther* 2011; **24**(3): 311-319.

40 Takahashi R, Kinoshita-Ise M, Yamazaki Y, Fukuyama M, Ohyama M. Increase in CD8(+) Effector Memory T Cells Re-Expressing CD45RA Correlates with Intractability of Severe Alopecia Areata. *J Invest Dermatol* 2024; **144**(7): 1654-1657 e1657.

41 Borcherding N, Crotts SB, Ortolan LS, Henderson N, Bormann NL, Jabbari A. A transcriptomic map of murine and human alopecia areata. *JCI Insight* 2020; **5**(13).

42 Lee EY, Dai Z, Jaiswal A, Wang EHC, Anandasabapathy N, Christiano AM. Functional interrogation of lymphocyte subsets in alopecia areata using single-cell RNA sequencing. *Proc Natl Acad Sci U S A* 2023; **120**(29): e2305764120.

43 Duquette D, Harmon C, Zaborowski A et al. Human Granzyme K Is a Feature of Innate T Cells in Blood, Tissues, and Tumors, Responding to Cytokines Rather than TCR Stimulation. *J Immunol* 2023; **211**(4): 633-647.

44 Seok J, Cho SD, Lee J et al. A virtual memory CD8(+) T cell-originated subset causes alopecia areata through innate-like cytotoxicity. *Nat Immunol* 2023; **24**(8): 1308-1317.

45 El Aziz Ragab MA, Hassan EM, El Niely D, Mohamed MM. Serum level of interleukin-15 in active alopecia areata patients and its relation to age, sex, and disease severity. *Postepy Dermatol Alergol* 2020; **37**(6): 904-908.

46 Ebrahim AA, Salem RM, El Fallah AA, Younis ET. Serum Interleukin-15 is a Marker of Alopecia Areata Severity. *Int J Trichology* 2019; **11**(1): 26-30.

Abstract in Korean

활성기 원형탈모 환자의 혈액 내 NKG2D 양성 세포독성림프구의 면역학적 변화 분석

원형탈모(alopecia areata, AA)는 반복적인 모낭의 면역관용 붕괴로 인해 발생하는 만성 재발성 자가면역 질환이다. 면역관용의 붕괴는 NKG2D 리간드들의 발현으로 이어지며, 면역세포들의 공격으로 이어진다. 원형탈모의 병인 세포로는 NKG2D+ CD8 T 세포가 알려져 있으며, 이는 주로 마우스 모델을 통해 밝혀졌다. 인체에서도 NKG2D+ CD8+ T 세포의 역할이 확인되었으나, 인간과 동물 간 NKG2D 발현 양상의 차이가 존재하여 추가적인 연구가 필요하다.

최근 연구들은 원형탈모가 단순히 모낭에서 국한된 변화가 아니라 전신적인 면역체계 변화와 연관된 질환임을 밝혀지고있다. 선행 연구에서 혈액 내 면역학적 변화를 확인하였으며, 이러한 혈액내 변화가 두피의 변화와 상응 한다는 결과가 보고되었다. 다른 연구에서는 건강한 대조군과 비교했을 때 원형탈모 환자의 혈액 내 NKG2D+ CD4+, CD8+, NK 세포 비율 변화를 관찰하였다. 또한 백신 접종, 바이러스 감염, 알레르기 등의 환경적 요인이 원형탈모의 임상 양상에 영향을 미칠 수 있음이 보고되었다.

따라서 본 연구에서는 혈액 내 NKG2D+ 세포가 원형탈모의 임상적 경과에 따라 면역학적 변화를 보일 것이라 가정하고, 보다 정밀한 수준에서 이들 세포를 규명하고자 하였다. 또한, 기존 연구들에서 혈액내 면역세포의 임상적 특징과의 관련성은 명확히 밝혀지지 않았으므로, 이와의 관련성을 평가하고자 하였다. 먼저, NKG2D+ 세포의 발현과 원형탈모의 중증도 및 활성도와의 관련성을 확인하기 위해 건강한 대조군과 비교하여 말초혈액 단핵세포(PBMC) 내 면역세포를 분석하였다. CD4+, CD8+, NK (CD3- CD56+), CD3+CD56+ 세포군으로 나누어 비교했으나, 원형탈모 환자군과 건강한 대조군 간 유의미한 차이는 확인되지 않았으며, NKG2D+ 세포의 비율 또한 질환의 중증도나 활성도와 관련성이 없었다.

면역세포의 개인차를 고려하여, 후속 연구에서는 동일한 환자의 활성기와 안정기 상태를 비교하는 paired 분석을 진행하였다. NKG2D+ 세포에 초점을 맞춰 단일세포전사체 분석(single-cell RNA sequencing, scRNA-seq)을 수행한 결과, 혈액 내 NKG2D 발현 세포는 CD8+ T 세포, NK 세포, 점막연관불변 T(MAIT) 세포, γδ T 세포의 네 가지 주요 세포군으로 구성됨을 확인하였다. 원형탈모 활성기에서는 NKG2D+ 세포 중 NK 세포의 비율이 증가하고 CD8+ T 세포의 비율이 감소하는 경향을 보였다. CD8+ T 세포 내에서는 특징적으로 세포독성을 나타내는 GZMK+ 및

GZMB+ CD8+ T 세포가 활성기에 증가하였다. 이러한 변화는 MILO 를 이용한 차등 풍부도 분석 (differential abundance) 에서도 확인되었으며, 유세포분석에서도 일관된 결과를 보였다.

T 세포의 전사체 변화를 경로 분석(pathway analysis)을 통해 확인한 결과, 활성화 및 세포독성이 증가한 것으로 나타났다. T 세포의 변화를 유도하는 요인을 규명하기 위해 Ingenuity Pathway Analysis (IPA)를 이용한 상위 신호 분석을 수행한 결과, IL-15 와 같은 사이토카인이 주요 조절자로 확인되었다. 그러나 ELISA 를 통한 사이토카인 정량분석과 단핵구의 RNA 시퀀싱를 진행한 결과, 이러한 상위조절자의 활성기와 안정기 간 유의미한 차이는 확인되지 않았다.

본 연구를 통해 NKG2D+ 림프구의 전체적인 비율은 원형탈모 환자와 건강한 대조군 간, 그리고 질병의 중증도 및 활성도와의 관련성에서 유의미한 차이를 보이지 않았다. 그러나 단일세포전사체 분석을 통해 질병 활성기에 따라 특정 면역세포군의 비율이 변화하는 양상을 새롭게 확인하였다. 특히, NKG2D+ CD8+ T 세포의 비율이 감소하는 반면, 세포독성을 지닌 CD8+ T 세포가 증가하는 특징이 확인되었다. 다만, 이러한 면역변화를 유도하는 상위 조절자로 확인된 사이토카인의 활성기 혈액 내 증가는 확인되지 않았다. 따라서, 향후 추가 연구를 통해 혈액내 면역학적 변화를 유도하는 기전을 규명할 필요가 있을 것으로 생각된다.

핵심되는 말 : 원형탈모, NKG2D, 세포독성 T 세포